

# Sentinel-2 data processing and identifying glacial features in Sentinel-2 imagery

---

Ruben Egbers

Bachelor Thesis

TU Delft, University of Technology

July 2016

Supervisors: Dr. R.C. Lindenbergh, Dr. M. Vizcaino

## Table of Contents

List of abbreviations.....	iv
Abstract .....	v
<b>1. Introduction .....</b>	<b>1</b>
1.1 Research question.....	1
<b>2. Research content .....</b>	<b>3</b>
2.1 Glaciers in the Hindu-Kush Himalayan .....	3
2.2 Remote sensing and spectral data.....	4
2.3 Climate and glaciers in the Hindu-Kush Himalayan region .....	6
<b>3. Datasets .....</b>	<b>8</b>
3.2 Sentinel-2 product.....	9
3.2.1 Level-1B.....	9
3.2.2 Level-1C.....	9
3.2.3 Level-2A.....	9
3.2.4 Product naming and format.....	11
3.3 ASTER GDEM .....	13
3.4 GLIMS glacier mask.....	13
3.5 Landsat 8 .....	14
<b>4. Methods .....</b>	<b>16</b>
4.1 Data and software selection.....	16
4.1.1 Data selection.....	16
4.1.2 Software selection .....	17
4.2 Sentinel-2 data processing .....	18
4.2.1 Scene classification .....	18
4.2.2 Atmospheric correction .....	20
4.3 Landsat 8 data processing .....	20
4.4 Snowline detection.....	21
4.5 Superimposing ASTER GDEM v2 with Sentinel-2 data .....	21
4.6 NDSI .....	22
4.7 Band combinations .....	23
4.8 Spectral information of snow and ice in Sentinel-2 data.....	24
<b>5. Results .....</b>	<b>25</b>
5.1 Data processing results.....	25
5.2 Sentinel-2 compared with Landsat 8.....	27
5.3 Snow/ice mapping with band combinations.....	31
5.4 Snowline determination .....	34
<b>6. Discussion .....</b>	<b>36</b>
6.1 Processing problems.....	36
6.2 Differences between the first and second Sentinel-2 dataset.....	37
6.3 Comparison between Landsat 8 and Sentinel-2.....	37
6.4 Differences between band combinations.....	38
6.5 Snowline determination .....	38
6.6 GLIMS as an incomplete dataset .....	38
<b>7. Conclusion .....</b>	<b>39</b>
<b>8. Recommendations .....</b>	<b>40</b>
<b>References .....</b>	<b>41</b>

<b>Appendix 1: Data processing and images .....</b>	<b>44</b>
<b>Appendix 2: Zoomed in images of snowlines .....</b>	<b>46</b>

## List of abbreviations

AOT	Aerosol Optical Thickness
ASTER	Advanced Spaceborne Thermal Emission and Reflection Radiometer
BOA	Bottom of Atmosphere
(G)DEM	(Global) Digital Elevation Model
DN	Digital Number
DOS	Dark Object Subtraction
ELA	Equilibrium-Line Altitude
GLIMS	Global Land Ice Measurements from Space
MODIS	Moderate Resolution Imaging Spectroradiometer
(V)NIR	(Visible and) Near Infrared
NDSI	Normalised-Difference Snow Index
NN	Neural Network
S2AC	Sentinel-2 Atmospheric Correction
SC	Scene Classification
SNAP	Sentinel Application Platform
SWIR	Shortwave Infrared
TIR	Thermal Infrared
TOA	Top of Atmosphere
TS	Threshold algorithm
UTC	Coordinated Universal Time
UTM	Universal Transverse Mercator
WGS84	World Geodetic System 1984

## Abstract

The goal of this study is to investigate how Sentinel-2 images are processed and if these images are useful to study glacial features like snowlines. The study location is the Karakoram mountain range on the western part of the Tibetan Plateau. A lot of glaciers are contained within this region, which has the interesting property that glaciers are expanding here, instead of retreating while the Earth is getting warmer.

In this study, methods are explored to process Sentinel-2 images. Other datasets that have been used to investigate the properties of Sentinel-2 are Landsat 8, ASTER GDEM v2 and the GLIMS glacier mask. The processing of Sentinel-2 data was done in the Sentinel-2 Toolbox of ESA. Several different methods were then used in order to determine snowlines on glaciers in the area, by using ASTER GDEM v2 and the GLIMS glacier mask. Besides from being distinguished visually with different band combinations, snow and ice can also be distinguished from other types of land cover by using the Normalised-Difference Snow Index (NDSI). This is a ratio of the spectral response of snow in the visible and near-infrared/shortwave infrared part of the electromagnetic spectrum.

Sentinel-2 data that was obtained just after the start of the mission had several issues with shadows and oversaturation due to the wrongly calibrated sensors at the time. New Sentinel-2 imagery proved to be an excellent tool to study glaciers in great detail, with a considerably higher spatial resolution compared to Landsat 8. The snowlines that were determined coincided well with already available literature and other glacial features were clearly visible on the Sentinel-2 images, making the combination of Sentinel-2 and Landsat 8 an excellent way of monitoring glaciers in detail. It could be interesting to look at seasonal variation in snowlines of the Karakoram glaciers in future research, to further investigate the Karakoram anomaly.

## 1. Introduction

Sentinel-2 is a satellite operated by the European Space Agency and became operational in late 2015. It collects spectral information during its orbit around the earth. This type of satellite imagery can be used to determine changes in land cover, such as retreating or advancing glaciers. The Tibetan plateau contains a large amount of glaciers and is therefore interesting to research in times of a changing climate. Most of the areas are remote and difficult to access, which makes remote sensing techniques an excellent solution to observe changes.

The location of the study was supposed to be the Nyainqêntanlgha mountain range, but this was impossible due to a lack of data. Therefore, the location was changed to the Karakoram mountain range, which includes several long glaciers such as the Baltoro glacier or the Hispar glacier. It includes several 8000+ m mountains (K2, Gasherbrum I and Gasherbrum II). The area is shown in figure 1 within the blue box. Glaciers in the Karakoram are not retreating, but they gain mass (Hewitt, 2005), making this an interesting study area. The goal is to see if and how Sentinel-2 data can be used in order to study the glaciers in this area. In order to do this, the data needs to be processed first. From there several possibilities were explored to map and distinguish snow and ice on these images. Once this was done, Sentinel-2 images were compared with Landsat 8 satellite images and snowlines were extracted from the images. If snowlines are determined during dry season, with low snowfall, they approximate the Equilibrium Line Altitude of the glacier, which says something about the state of the glacier (see section 2.1). Also, attention was paid to the individual features of a glacier and to what potential Sentinel-2 has to map these features, compared with Landsat 8.

This study is structured as follows. Chapter 2 covers general information on glaciers, remote sensing and the regional climate. The used datasets are described in chapter 3 followed by the methods in chapter 4. The results are given in chapter 5 and the results are discussed in chapter 6. This is followed by the conclusion in chapter 7 and finally, the recommendations in chapter 8.

### 1.1 Research question

The main goal of this research is to find out how Sentinel-2 data can be used and if it is useful for glacial research in the Karakoram.

Several subquestions are:

- How is Sentinel-2 data processed?
- How does Sentinel-2 data compare to Landsat 8 data?
- Is it possible to extract snowlines from Sentinel-2 imagery and how is this done?
- Is it possible to distinguish other glacial features from Sentinel-2 data?

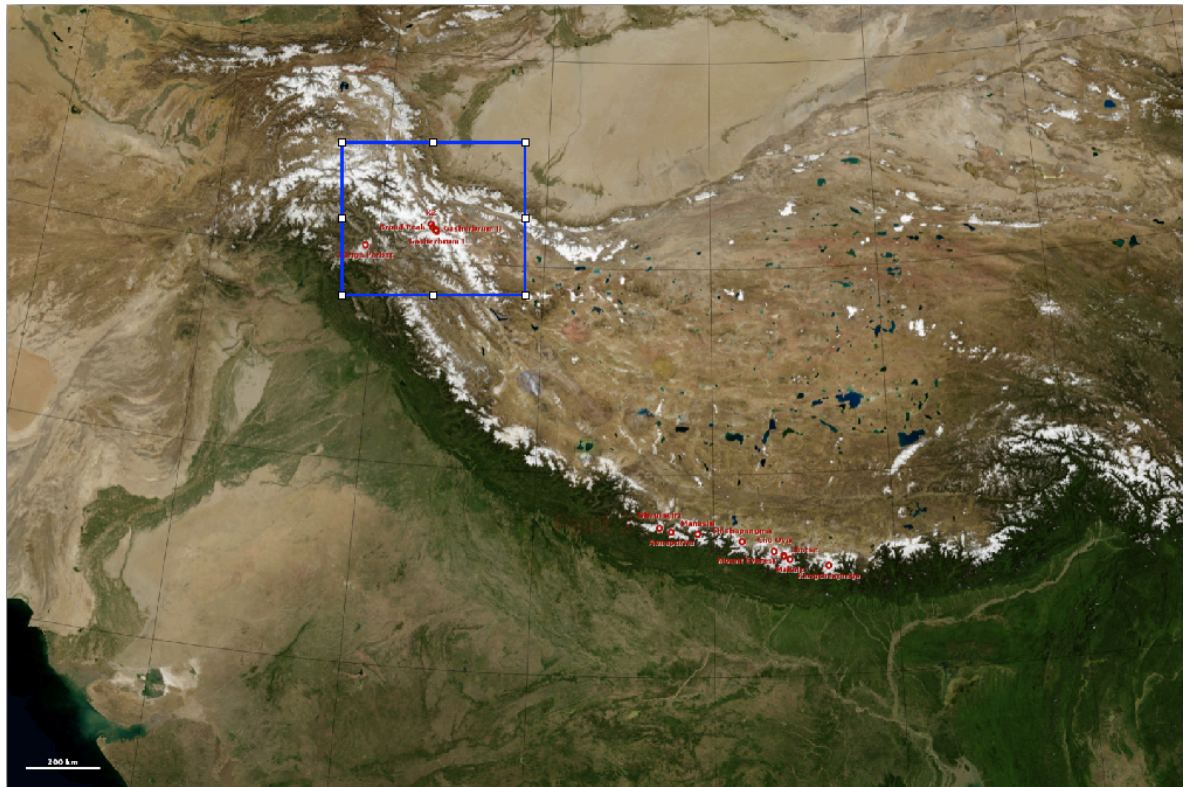
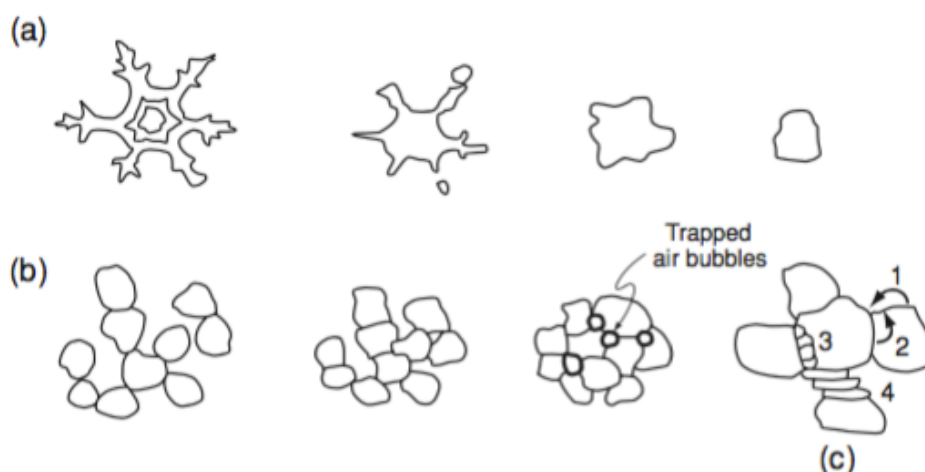


Figure 1: Location of the study area in blue, scale in the lower left of the image is 200 km (modified from NASA).

## 2. Research content

### 2.1 Glaciers in the Hindu-Kush Himalayan

A glacier is a massive body of dense ice, which is constantly moving due to gravity. They can grow and shrink throughout the years when snow falls and accumulates on a glacier. Snow that accumulates on the glacier gradually transforms into ice, as shown in figure 2.



**Figure 2: Transformation of snow into ice. (a) Modification of snow flakes to a subspherical form. (b) Sintering. (c) Processes during sintering: 1 = sublimation, 2 = molecular diffusion within grains, 3 = nucleation and growth of new grains and 4 = internal deformation of grains (Hooke, 2005).**

Glaciers can be covered in snow, when this has not been transformed into ice yet. If this is the case, the glacier will be affected in a different way than if it was not covered with snow. This has to do with the value of the albedo of snow, which is higher than the albedo of ice. The albedo is the percentage of radiation that is reflected from a surface and thus has a value between 0 and 100 % (or between 0 and 1, if it is a ratio). Typical albedo values are presented in table 1. It is clear that snow has quite a variable range of albedo, as snow can be fresh or dirty, where dirty snow will have a lower albedo than fresh snow. Dry snow, with an albedo up to 97 %, is almost a perfect reflector and ice is not a good reflector or absorber, since its albedo ranges from 10-51 percent, depending on how clean the ice is.

**Table 1: Albedos for snow and ice (Benn & Evans, 1998).**

	Range (%)	Mean (%)
<b>Dry snow</b>	80-97	84
<b>Melting snow</b>	66-88	74
<b>Firn</b>	43-69	53
<b>Clean ice</b>	34-51	40
<b>Slightly dirty ice</b>	26-33	29
<b>Dirty ice</b>	15-25	21
<b>Debris-covered ice</b>	10-15	12

From this it is clear that there will be a boundary on a glacier, between snow and ice. This boundary is called the snowline. Snowlines can vary throughout a year, especially in the dry and wet season, when snow cover will decrease or increase, respectively. The definition of the Equilibrium-Line Altitude or ELA is the elevation/area on a glacier where accumulation equals ablation over a 1-year period (Singh, Singh, & Haritashya, 2011). The snowline can be a good approximation of the ELA in the dry season, when there is minimum precipitation. Thus, a glacier can retreat or advance, but this is dependent whether there is net accumulation or ablation. The accumulation area is the upper elevation zone where there is an annual net gain in mass. The ablation area, in contrary, is the lower elevation zone where there is a net annual loss in mass (National Research Council, 2012). A schematic of a glacial mass balance like this is given in figure 3.

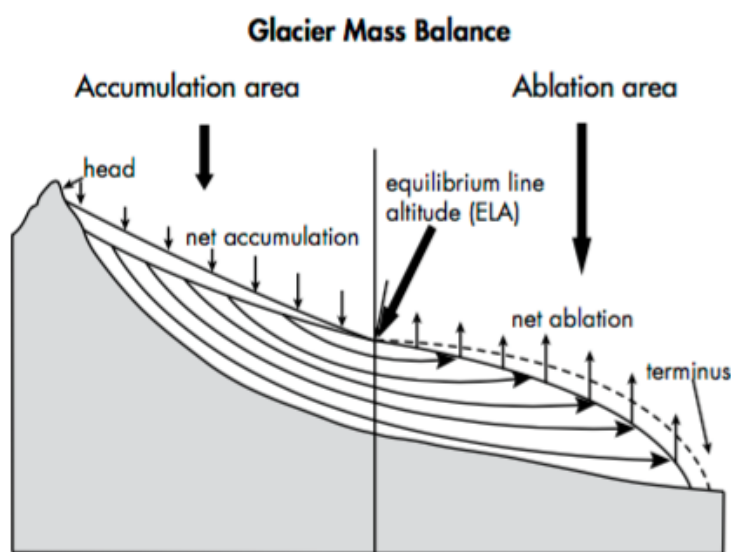


Figure 3: Glacier accumulation and ablation areas, including the ELA (Armstrong, 2010)

## 2.2 Remote sensing and spectral data

In remote sensing, methods are used to obtain information about an object without making any direct contact with the objects. There is a broad range of different methods to do this, however the focus in this study will be on satellite data that contains information of the electromagnetic radiation that is reflected/absorbed by the earth's surface. Every type of land cover has a typical spectral signature, meaning that they absorb/reflect radiation in a different region of the electromagnetic spectrum. Sentinel-2 has 13 bands that register the spectral signature of an area. For example, snow and ice can be distinguished from rock/vegetation/water by its spectral signature. A typical response is shown in figure 4.

However, clouds can be a problem when detecting snow cover, since clouds have similar spectral signatures. The bands located in the SWIR (Shortwave Infrared) part of the spectrum can be used to distinguish snow from other bright reflecting surfaces, given that snow has a low reflectance in this part of the spectrum. Besides cloud cover, sufficient daylight is also necessary to detect snow. Short wave and thermal infrared data combined with visible channels can be used to differentiate clouds from snow (WMO CHy-14, 2012).

The high response in the visible part of the spectrum is due to the high albedo and white colour of snow. Several factors that can cause a misidentification for snow are thus: clouds, forest cover, shadows and rocks (Eumetrain, 2016).

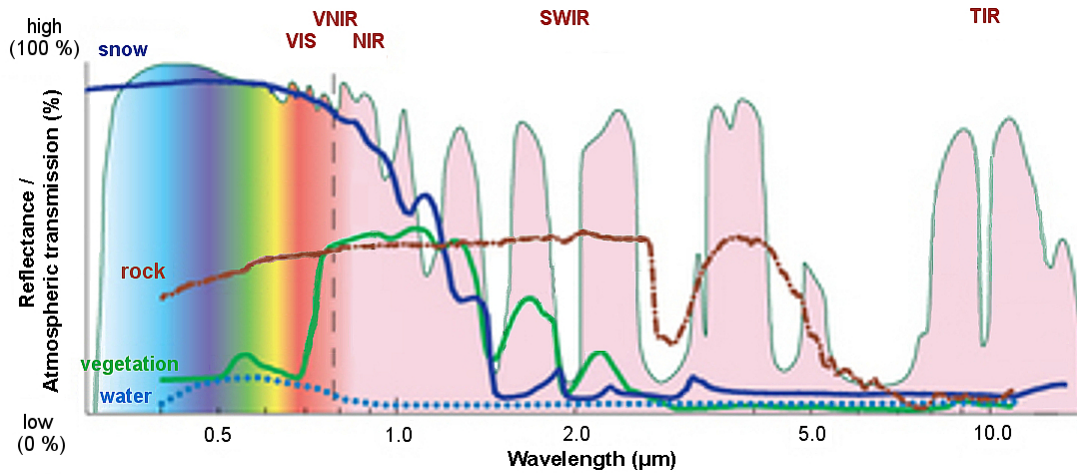


Figure 4: Reflectance/Transmittance response of different land covers (Eumetrain, 2016)

Different terms apply to spectral measurements with satellites. The individual pixels get assigned a Digital Number or DN. This is a pixel value that has not been converted to a physically meaningful unit. It might be sufficient not to convert this DN into a physically meaningful unit, such as radiance or reflectance. Radiance is the amount of radiation coming from an area and it usually has units in the form of Watt per steradian per square meter ( $Ws^{-1}m^{-2}$ ) or if it is the spectral radiance (which is the radiance per unit frequency or wavelength) it get the form  $Wm^{-3}sr^{-1}$  or more commonly  $Wm^{-2}sr^{-1}nm^{-1}$ . Radiance includes reflected surface radiation, radiation that reflects from a neighbouring pixel and radiation that has been reflected from clouds above the pixels area.

Reflectance is the ratio of radiation striking a surface to the radiation reflected off that same surface. Materials (or different types of surfaces) can be identified by their reflectance spectra; therefore it is common to correct an image to reflectance for identification of surfaces. Top of atmosphere reflectance is the reflectance of a space-based sensor that orbits the earth outside the atmosphere. These reflectance values include disturbances of clouds, atmospheric aerosols and gases. Typically, one is interested in the bottom of atmosphere reflectance (also called surface reflectance). This is the reflectance of the Earths surface. Atmospheric corrections have been applied in this case. There are several different models to do this. The most accurate ones include the spectral line structure of molecules in the atmosphere and multiple scattering and/or polarisation effects (Rees, 2013). Another method is to calibrate the sensors to targets of known reflectance. The last method is the simplest method, and the most applied method of atmospheric correction and it is based on dark-pixel subtraction. The minimum radiance pixel is identified for each band in the image and the minimum radiance is then subtracted from all pixels in the image (Rees, 2013).

### 2.3 Climate and glaciers in the Hindu-Kush Himalayan region

The region of interest, the Hindu-Kush-Himalayan, extends over 2000 km east to west, crossing Afghanistan, Bangladesh, Bhutan, China, Pakistan, India, Myanmar and Nepal, as seen in figure 5.



Figure 5: The Hindu-Kush Himalayan region shown in dark green (Himalayan glaciers : climate change, water resources, and water security, 2012)

The variation in elevation in this area is great, from the base of the Indo-Gangetic Plain near sea level to the great mountains of the Tibetan Plateau/Karakoram (7000-8000 m). A typical phenomenon in this area is the monsoon, depending on the location of study. The monsoon is a seasonal reversing wind, which is accompanied by changes in precipitation rates.

The climate varies greatly in the area, from tropical at lower elevations to permanent ice and snow conditions at higher elevations. In spring and late summer, India and Bangladesh experiences monsoon rain. In winter the direction reverses, causing the area to be relatively dry. Most of the precipitation in the Tibetan Plateau falls in winter, in the form of snow. The Karakoram mountain range has a very variable climate. Bolch (Bolch et al., 2012) stated that about two-thirds of the high-altitude snowfall in the western part of the Karakoram is due to the mid-latitude Westerlies, whereas in the east part of the Karakoram more than 80% of the precipitation falls during the summer monsoon. The study area is located in the Central Karakoram (including Hispar and Baltoro glacier). The monsoon and ELAs in the area are shown in figure 6. A rough estimate of the height of the ELAs in the area can be made from this figure. The ELAs in the area in this study are expected at an altitude of approximately 5000 m, which is a rough estimate made from figure 6.

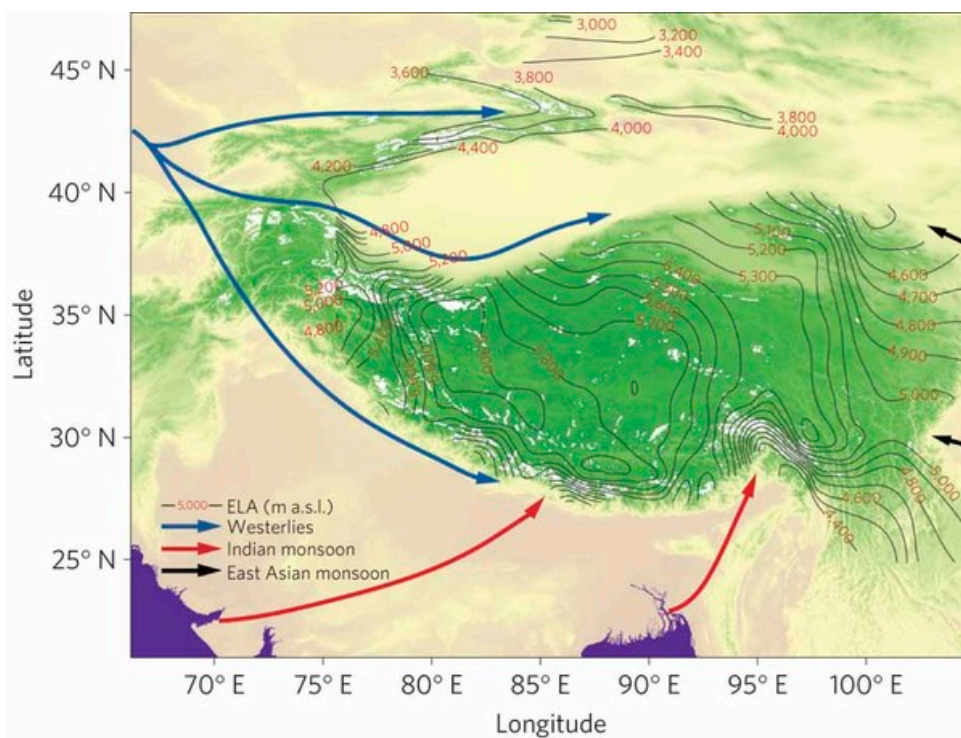


Figure 6: Monsoon in the area, the contour lines indicate the height of the ELAs (Yao et al., 2012)

### 3. Datasets

All data that has been used in this research is freely available online. Optical satellite images have been used from Sentinel-2, which is explained in section 3.1 and 3.2. Other data that has been used comes from the ASTER GDEM, explained in section 3.3, followed by the GLIMS glacier mask in section 3.4. Finally, Landsat 8 will be discussed in section 3.

#### 3.1 Sentinel-2

Sentinel-2 is a multi-spectral imaging mission, which supports the Copernicus Land Monitoring studies. The launch of Sentinel-2A on 23 June 2015 was the start of the Sentinel-2 programme and it will be followed by the launch of an identical satellite, Sentinel-2B, at the end of 2016 (expected launch at the time of writing). The revisit time of one single satellite is 10 days and for the combined constellation the revisit time will be 5 days, making it a good tool for time series studies. The coverage of the Sentinel-2 mission covers all continental land areas between latitudes 56° south and 83° north, all coastal waters up to 20 km from the shore, all islands which have a greater area than 100 km<sup>2</sup>, all EU islands. This is also shown in figure 7.

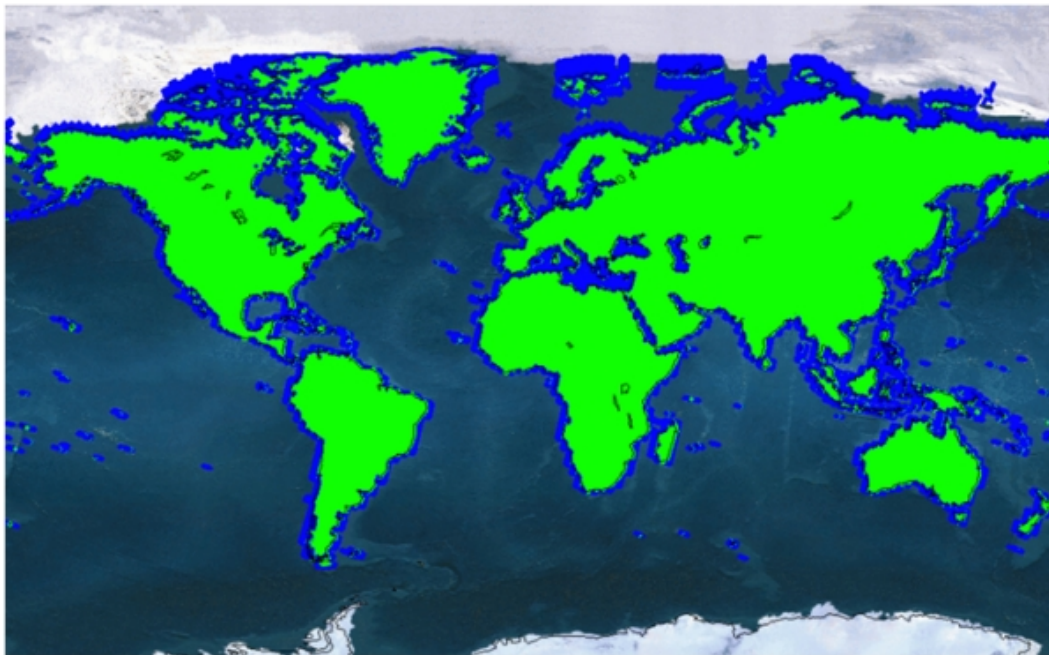


Figure 7: Sentinel-2 coverage at full operation (ESA, 2016)

The applications for the Sentinel mission are wide-ranged; most of them are related to the Earth's land surface and coastal zones. Several examples include:

- Spatial planning
- Environmental monitoring
- Water monitoring
- Forest and vegetation monitoring
- Crop monitoring

- Glacier monitoring, ice mapping, snow cover monitoring

## 3.2 Sentinel-2 product

The Sentinel-2 Multispectral Instrument (MSI) consists of 13 spectral bands at different spatial resolutions, noted in table 2 and visualised together with the Landsat 7 & 8 bands in figure 9. The MSI products are given in granules of a fixed size. There are several different types of product files available and the granule size depends on the product type. The following product types are distinguished: Level-0, Level-1A, Level-1B, Level-1C and Level-2A. Level-0 and Level-1A are not made available to users. Level-1A products are the result of decompressing the raw Level-0 data. The least processed product type that is made available to users is Level-1B. All data is freely available online at the Sentinels Scientific Data Hub (<https://scihub.copernicus.eu/>) as part of the Copernicus programme.

### 3.2.1 Level-1B

A level-1B product contains several granules that are 25 km across track and 23 km along track. Each granule is approximately 27 MB and is presented in \*.jp2 format. A \*.jp2 (JPEG-2000) file means that it is compressed following the JPEG-2000 standards. The product delivers radiometrically corrected TOA radiance values in sensor geometry. It also includes the geometric model, which is necessary to obtain the Level-1C product. The geometric model takes the motion of the satellite and the earth into account and it also predicts when the satellite and tracking stations can communicate (Floudas & Pardalos, 2009). The radiometric corrections that are applied to a Level-1B product are: dark signal, pixel response non-uniformity, crosstalk correction, defective pixel interpolation, high spatial bands restoration (deconvolution plus denoising) and binning for 60m bands (ESA, 2016). Crosstalk is a phenomenon in electronics by which a signal from one channel creates an unwanted effect in another channel.

### 3.2.2 Level-1C

A Level-1C product consists of 100 km<sup>2</sup> (orthorectified) images in UTM/WGS84 projection. This product is the result of using a DEM to project the image. The measurements that are provided per pixel are TOA reflectances with the necessary parameters to transform the reflectances into radiances. Level-1C products are resampled with a constant Ground Sampling Distance, which depends on the size of the band. Pixel coordinates refer to the upper left corner of the pixel. This product also contains Land/Water and Cloud masks and data that contains information on the total column of ozone/water vapour and the mean sea level pressure. Each tile is approximately 500 MB large.

### 3.2.3 Level-2A

A Level-2A product is also divided in tiles of 100 km<sup>2</sup>, which are approximately 600 MB large. The tiles are projected in UTM/WGS84. This type of product contains BOA reflectance images, which are derived from Level-1C products. This product type is not systematically generated, like all previous product types, but it has to be generated on the users side by using the Sentinel-2 Toolbox. This

will be discussed in more detail in section 4.2. The difference of a Level-2A product in comparison with a Level-1C product is seen in figure 8.



Figure 8: Level-1C product (left, TOA) and a Level-2A product (right) (ESA, 2016); location unknown.

Table 2: Sentinel-2 bands with spatial resolution, bandwidth and location in the electromagnetic spectrum. (ESA, 2016)

Band number	Resolution (m)	Central wavelength (nm)	Bandwidth (nm)	Part of spectrum	Description
1	60	443	20	Visible/VNIR	Coastal aerosol
2	10	490	65	Visible/VNIR	Blue
3	10	560	35	Visible/VNIR	Green
4	10	665	35	Visible/VNIR	Red
5	20	705	15	VNIR	Vegetation (red edge)
6	20	740	15	VNIR	Vegetation (red edge)
7	20	783	20	VNIR	Vegetation (red edge)
8	10	842	115	VNIR	NIR
8a	20	865	20	VNIR	Vegetation (red edge)
9	60	945	20	VNIR/SWIR	Water vapour
10	60	1375	30	SWIR	Cirrus
11	20	1610	90	SWIR	SWIR
12	20	2190	180	SWIR	SWIR

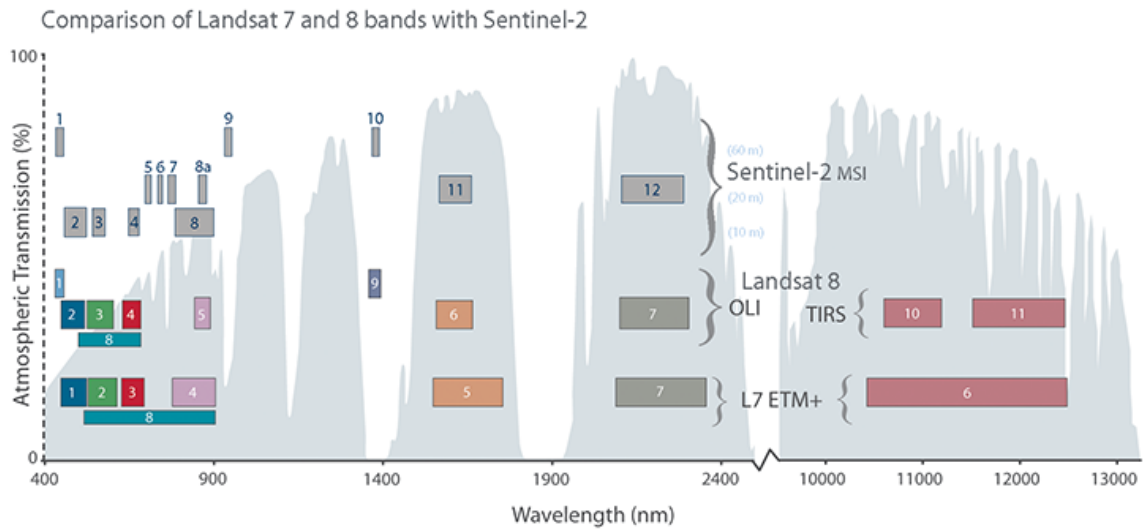


Figure 9: Landsat 7 & 8 bands compared with Sentinel-2 bands (NASA, 2016)

### 3.2.4 Product naming and format

When a Sentinel-2 product is downloaded, the folder name is rather confusing, therefore it will be explained here. It starts with the mission identifier (MMM), which can be S2A or S2B, depending on which satellite acquired the data (at the time of writing, only Sentinel-2A is in orbit and Sentinel-2B has not been launched yet). It is followed by the file class, which will be OPER, because the satellite is functional. It could also be TEST, if the satellite is still in its test phase. This is followed by the file type, which can be any of the levels indicated at TTTTTTTTTT in figure 10. It allows characterising the product level. Then, the site centre (ssss) gives information on the processing facility. It can be any site shown at (ssss) in figure 10. The creation date is then given in UTC (Coordinated Universal Time), followed by the relative orbit number (ROOO). Then the applicability time period is given: it begins with the moment when sensing begins and ends with the sensing time stop moment.

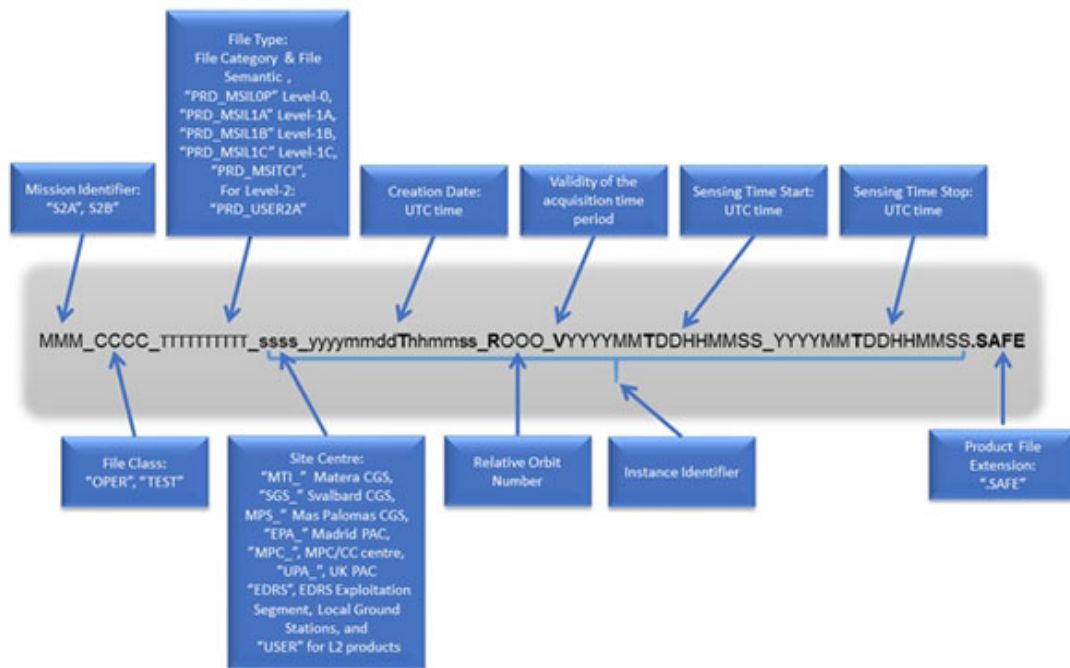


Figure 10: Product naming convention (ESA, 2016)

The product itself consists of different granules, which have their own naming conventions, as seen in figure 11. This is similar to the product naming convention and therefore shall not be evaluated in the same detail.

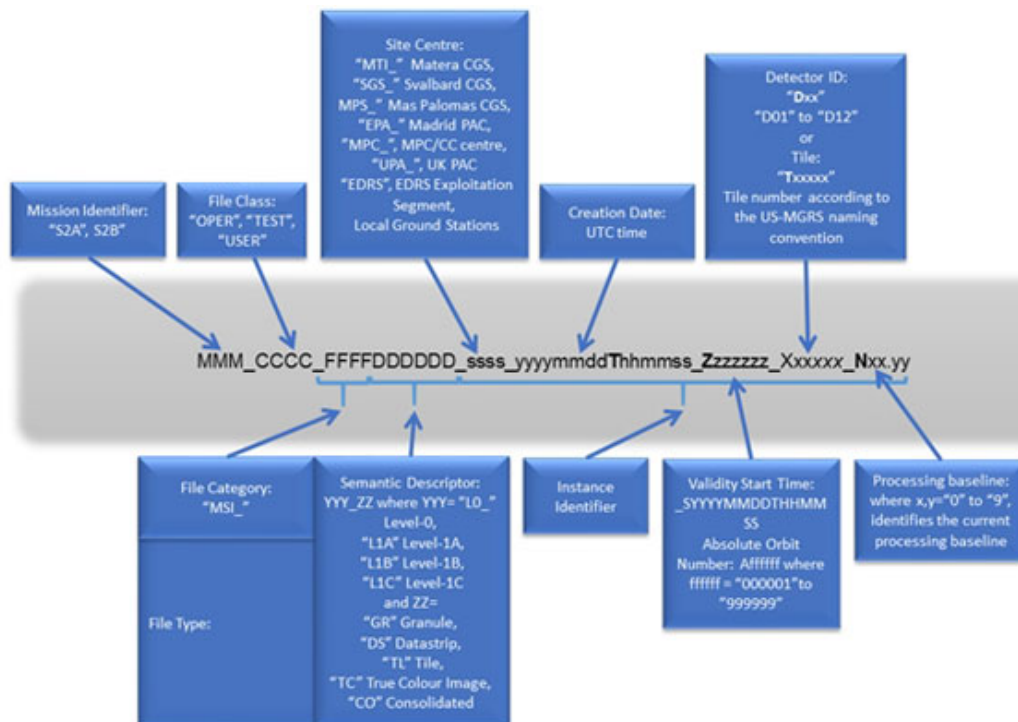


Figure 11: Granule tile naming convention (ESA, 2016).

### 3.3 ASTER GDEM

ASTER (short for Advanced Spaceborne Thermal Emission and Reflection Radiometer) is an instrument aboard the Terra spacecraft, which was launched into a sun-synchronous orbit around Earth on December 18, 1999. ASTER contains several sub-instruments: the VNIR, SWIR and TIR subsystem, respectively. It was built for a wide variation of scientific research; from hazard monitoring to land surface and land cover change. Part of the mission was to create a DEM, the latest version was released on October 17, 2011 (GDEM V2). This was done by using stereo-pair images that were collected by ASTER, as shown in figure 12. The coverage of ASTER GDEM spans from 83 degrees north latitude to 83 degrees south, which is approximately 99 % of the Earth's surface (NASA, 2016) with a resolution of 30m. This is done by apply photogrammetry to all collected ASTER scenes. The scenes are presented in 1°-by-1° tiles in GeoTiff format, referenced to the WGS84/EGM96 geoid. The data is available free of charge at <http://reverb.echo.nasa.gov/reverb/>. It should be noted that there are also alternative DEMs available, such as SRTM, which has a lower resolution (90 m) and a lower global surface coverage.

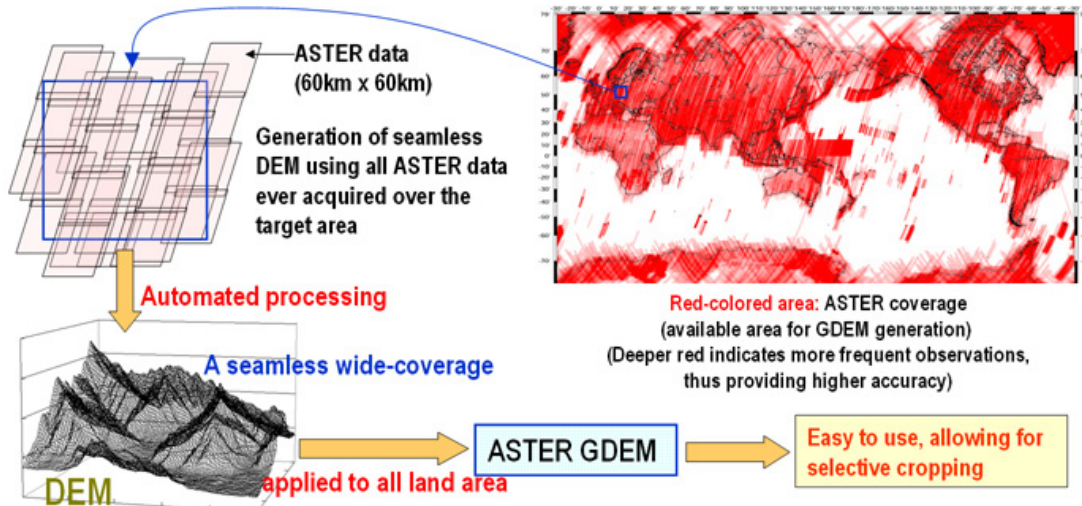


Figure 12: Concept of ASTER GDEM development (Jspacesystems, 2016)

### 3.4 GLIMS glacier mask

Another dataset used in this research is the GLIMS glacier mask. GLIMS stands for Global Land Ice Measurements from Space. This project aims to monitor the world's glaciers by using data from optical satellites. This is done by combining data from the ASTER instrument with data from Landsat missions. The products are available in different formats: KML (Google Earth viewing), ESRI shapefiles (QGIS and other GIS systems), GMT (Generic mapping tools), Mapinfo or GML (Geography Markup Language). It is freely downloadable from <http://www.glims.org/maps/glims> in an interactive map view. The GLIMS glacier mask is shown in figure 13. It is also immediately clear from this figure, that the GLIMS database is not complete. A missing glacier is pointed out with the red arrow.

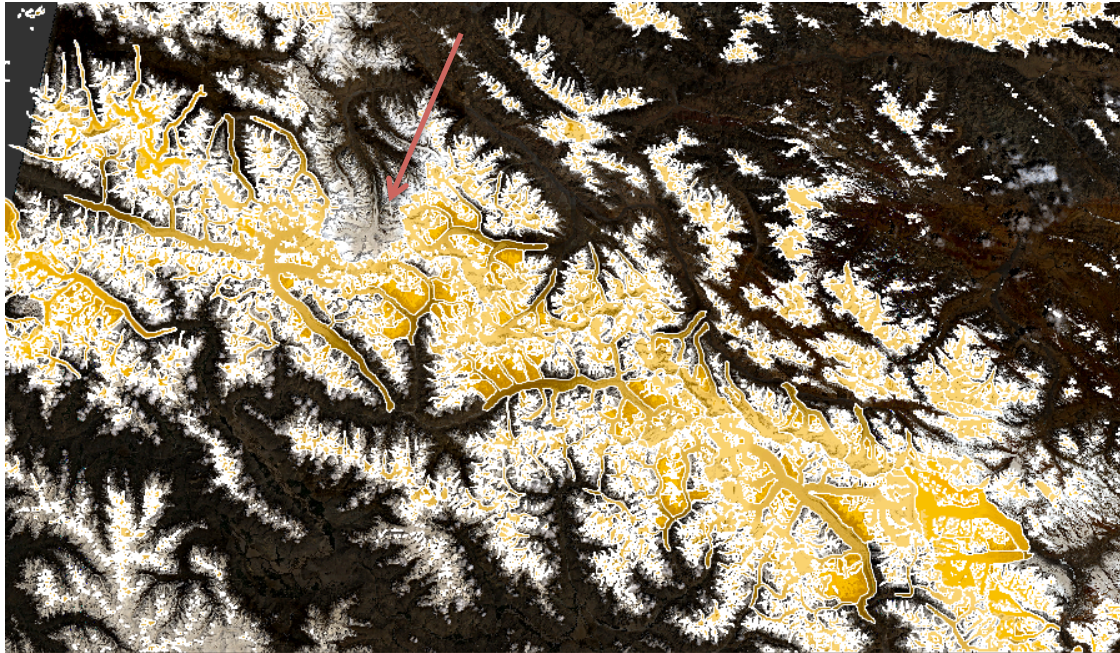


Figure 13: GLIMS superimposed on the Central Karakoram, zoom 1:306.2, missing glacier indicated with a red arrow

### 3.5 Landsat 8

Landsat is long-term project that started in 1972 and is run by NASA and USGS. Currently, Landsat 7 and Landsat 8 are still active. In this research, scenes acquired by the Landsat 8 mission will be used. Landsat 8 data is similar to Sentinel-2 data, meaning that it provides spectral data of a certain location at a certain time, however Landsat has got a different revisit time of 16 days. Landsat 8 contains 2 sensors: the Operational Land Image (OLI) and the Thermal Infrared Sensor (TIRS). A Landsat 8 image consists of nine spectral bands and are approximately 170 km (N-S) x 183 km (E-W). The bands and their resolutions are shown in table 3. Landsat 8 data is provided in GeoTiff format with a WGS 84/UTM projection and can be handled in both QGIS and the Sentinel-2 toolbox. The data is available for free online through EarthExplorer (Earthexplorer, 2016). The data is provided at different processing levels, similar to Sentinel-2 data. The data used here has level L1T, meaning that the raw data has been corrected for terrain. Atmospheric effects have not been corrected when the data is downloaded, but this can be done in QGIS, as explained in section 4.3.

An extra feature in the Landsat 8 data is that it also provides a Quality Assessment band (QA), which gives an indication of how useful a certain pixel is when it comes to surface, atmospheric and sensor conditions. This band is not used in this research as it requires more in depth understanding of the subject and it is not relevant, but it is be useful to see whether or not a dataset is suitable for the purpose of research.

**Table 3: Landsat 8 bands, wavelengths and their resolution (NASA, 2016)**

<b>Landsat 8 Operational Land Imager (OLI) and Thermal Infrared Sensor (TIRS)</b>	<b>Bands</b>	<b>Wavelength (nm)</b>	<b>Resolution (m)</b>
	Band 1 - Coastal aerosol	433 - 453	30
	Band 2 - Blue	450 - 515	30
	Band 3 - Green	525 - 600	30
	Band 4 - Red	630 - 680	30
	Band 5 - Near Infrared (NIR)	845 - 885	30
	Band 6 - SWIR 1	1560 - 1660	30
	Band 7 - SWIR 2	2100 - 2300	30
	Band 8 - Panchromatic	500 - 680	15
	Band 9 - Cirrus	1360 - 1390	30
	Band 10 - Thermal Infrared (TIRS) 1	10600 - 11200	100 * (30)
	Band 11 - Thermal Infrared (TIRS) 2	11500 - 12500	100 * (30)

\*TIRS bands are acquired at 100-meter resolution, but are resampled to 30 meter in delivered data product.

## 4. Methods

The methods used during the research are presented in this chapter. First of all, the process of data and software selection is explained in section 4.1. Followed by the methods of processing Sentinel-2 data to BOA reflectances in section 4.2 and Landsat 8 data in section 4.3. Snowline detection is treated in section 4.4, followed by the method used to extract snowlines in section 4.5. Section 4.5 contains the Normalised-Difference Snow Index (NDSI), while section 4.7 focuses on mapping snow and ice with different band combinations. Finally, section 4.8 deals with the spectral signatures of snow and ice.

### 4.1 Data and software selection

#### 4.1.1 Data selection

First of all, Sentinel-2 data has to be acquired. This is freely available online through the Copernicus programme of ESA, via <https://scihub.copernicus.eu/>. During the selection process, different areas have been considered such as the Khumbu glacier near Mount Everest, the Nyainqêntanglha Mountains and areas in the Karakoram mountain range. Nyainqêntanglha is interesting since there is already data available from an earlier study, however no usable Sentinel-2 data with decent cloud coverage is available at the time of writing. The same goes for the area of the Mount Everest. One dataset has been found of the Karakoram area, which includes the long Hispar glacier and a lot of other glaciers that are clearly visible even though the relatively high cloud coverage of approximately 46 %, as shown in table 4. This dataset is acquired just after the Sentinel-2A satellite became operational, because the first data that was shot dates from November 27, 2015 (can be found in the online sentinel-2 database). Another dataset was found from May 18, 2016 of roughly the same area, however this dataset is slightly different. The first Sentinel-2 dataset is projected in UTM42/43N and the second dataset is projected in UTM43/44N. The Landsat data that was found was selected in such a way that the acquisition dates were close to the Sentinel-2 data, however this was not always possible due to high cloud cover percentages, which made the image not usable.

Furthermore, it is also sensible to look at the time of year when the images are acquired. The reason for this is that in winter (or wet season, depending on the location), the glaciers will be covered in more snow due to high precipitation rates and/or cold temperatures. If the snowline is determined during dry season, this approximates the ELA of the glacier. However, the winter dataset was initially chosen because of the glaciers that are clearly visible and because it is also interesting to look at seasonal variation.

Table 4: Used datasets in this research

Date Time	Sensor / Product	Resolution (m)	Cloud coverage (%)	Source	Path/Row	Original product level	Size (GB)
3 December 2015 11:40:39	Sentinel-2A MSI	10/20/60	45.57	Scihub (ESA)	-	1C	7.15
18 May 2016 13:06:40	Sentinel-2A MSI	10/20/60	46.70	Scihub (ESA)	-	1C	7.77
29 April 2016	GLIMS mask	-	-	GLIMS	-	-	-
3 October 2011	ASTER	30	-	USGS	-	GDEM V2	-
26 May 2016	Landsat 8 OLI/TIRS	30	32.89	USGS	149/35	1T	1.81
4 June 2016	Landsat 8 OLI/TIRS	30	29.66	USGS	148/35	1T	1.78

#### 4.1.2 Software selection

In order to use the data one needs to have a programme which is familiar with \*.jp2 formats, since the Sentinel-2 raster data from ESA is presented in this format. QGIS is an open source GIS platform that can be used to read and manipulate the data, for example to stack data or manipulate the bands. However, the datasets are relatively large and consist of multiple granules with independent bands. This makes it cumbersome to work in QGIS, since it experiences crashing when one handles large datasets or it becomes a very slow and time-consuming process. Another option is to use the Sentinel-2 toolbox, available online from <http://step.esa.int/main/download/>, which is part of SNAP, the common architecture for Sentinel-1, -2 and -3 toolboxes. This programme contains a lot of tools to exploit the data from the MSI instrument of the Sentinel-2 mission. This is preferred for Sentinel-2 data as it is a lot quicker than QGIS and it does not crash as often. It is also possible to use Landsat 8 (or MODIS) data in the architecture of SNAP, but Landsat 8 data is presented in individual bands so it is preferred to use QGIS for manipulating Landsat 8 data to a single image file. This single image can then be used in both QGIS and the Sentinel-2 toolbox.

The Sentinel toolbox is currently still under development by Brockmann Consult, CS-Romania, Telespazio Vega Deutschland, INRA and UCL. SNAP 3.0.0 was used in this research, along with the Sentinel-2 toolbox that is part of it.

## 4.2 Sentinel-2 data processing

The goal of processing a Level-1C product to a Level-2A product is to convert TOA reflectances to BOA reflectances. This is not done systematically and therefore has to be done by the user. The user can choose to process the data at 10, 20 and 60m resolution according to the users preferences. For some applications it might not be necessary to use the Sen2Cor processor, for example if only TOA reflectance is needed. The process is split up and two parts: scene classification and atmospheric correction. The scene classification provides a classification map that shows land cover per pixel (see figure 14, scene classification figure). The atmospheric correction is done to transform TOA reflectance to BOA reflectance. This is done by algorithms, which have been developed by DLR/Telespazio and can be run from the Sentinel-2 Toolbox. The module is called Sen2Cor and has to be installed manually and depending on the operating system, it has to be run from Terminal (OSX) or regular user interface of the Sentinel-2 Toolbox. The Sen2Cor processor is also freely available online (<http://step.esa.int/main/third-party-plugins-2/sen2cor/>). To install the Sen2Cor processor, one needs to have a python library (such as Anaconda) installed on the operating system.

The algorithms have to be executed at the native resolution of the bands (either 10, 20 or 60m). For bands at a higher resolution, it is necessary to resample back to 60m in order to gain a classification map at that resolution. Therefore, once one starts processing the data, one has to start at a 60m resolution, followed by processing at 20m and finally ending at a 10m resolution Level-2A product.

Thus, all data has been processed at a 60m resolution, meaning that the bands with a resolution of 10m and 20m were resampled to 60m first. Then all bands with a resolution of 20 m were processed and finally the 10m bands were processed as well. This is done to create an image as accurate as possible, since it is not preferred to lose resolution by just processing at 60m. Note that this is a very time-consuming but necessary process. Processing to 10 m resolution can take up to 12+ hours, depending on the size of the image. Since the processor is Python based, it might be possible to automatise the process with a Python script. The version of Sen2Cor that was used is version 2.2.1.

### 4.2.1 Scene classification

The scene classification algorithm creates a classification map that contains 4 different cloud classes and six different classifications for shadows, cloud shadows, vegetation, soils/deserts, water and snow. It also gives a quality indication on cloud and snow probability. The algorithm is depicted in figure 15 and it becomes clear that there are three output products after the scene classification algorithm: a cloud quality index map, a snow quality index map and a classification map, which includes cirrus clouds. Before that, cloud/cirrus/snow has to be detected first. These quality indicators give the probability that clouds or ice/snow covers the surface. The classification map provided by this algorithm has a resolution of 60m.

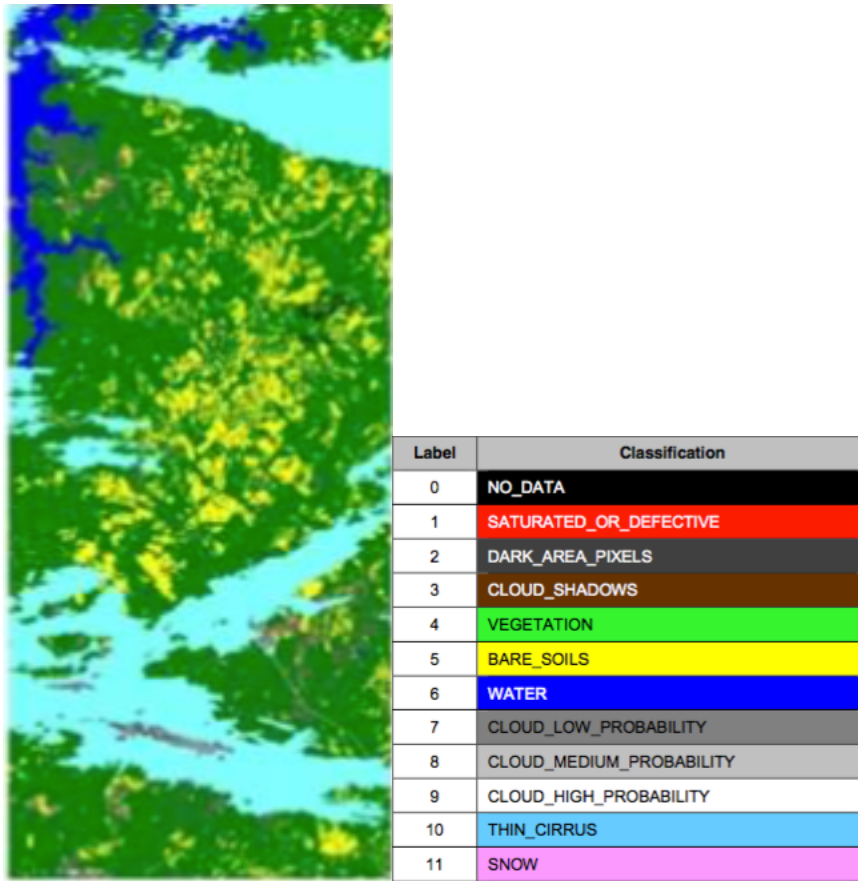


Figure 14: Scene classification (SC) map and legend (Müller-Wilm, 2016), as result of the SC algorithm of the Sen2Cor processor. The scene classification is of the same location as in figure 8.

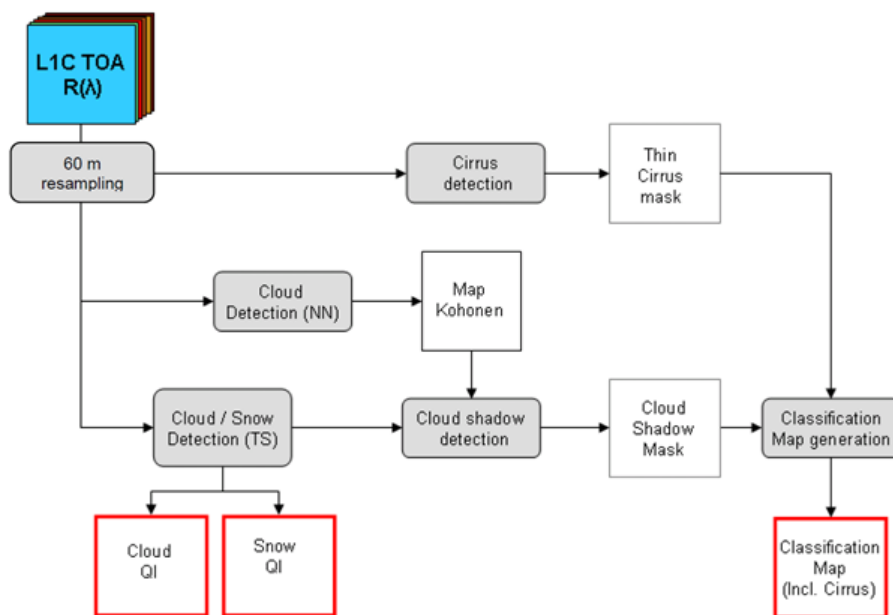


Figure 15: Scene classification algorithm containing the Level-2A processing modules (grey) and output products (red) (ESA, 2016)

### 4.2.2 Atmospheric correction

This algorithm converts a Level-1C (TOA) product to a Level-2A (BOA) product. According to ESA's website, this algorithm is based on the algorithms proposed in Atmospheric/Topographic correction for Satellite Imagery (ATCOR; Richter and Schlaepfer, 2011). This algorithm derives the Aerosol Optical Thickness (AOT), it retrieves the water vapour content and it also corrects for terrain. The processing flow for the S2AC algorithm is shown in figure 16.

The AOT gives an indication of how transparent the atmosphere is. This is done by correlating the reflectance band 12 (SWIR) with bands 4 and 2 (red and blue, respectively) (Müller-Wilm, 2016). The final product is an AOT map, showing the Aerosol Optical Thickness.

Furthermore, the algorithm also corrects for cirrus clouds, which give reflectance in band 10. Finally, the surface reflectance retrieval is performed for bands 1-12 and this results in Level-2A output after atmospheric correction. The difference between a Level-1C product and a Level-2A product is shown in an RGB colour image in figure 8.

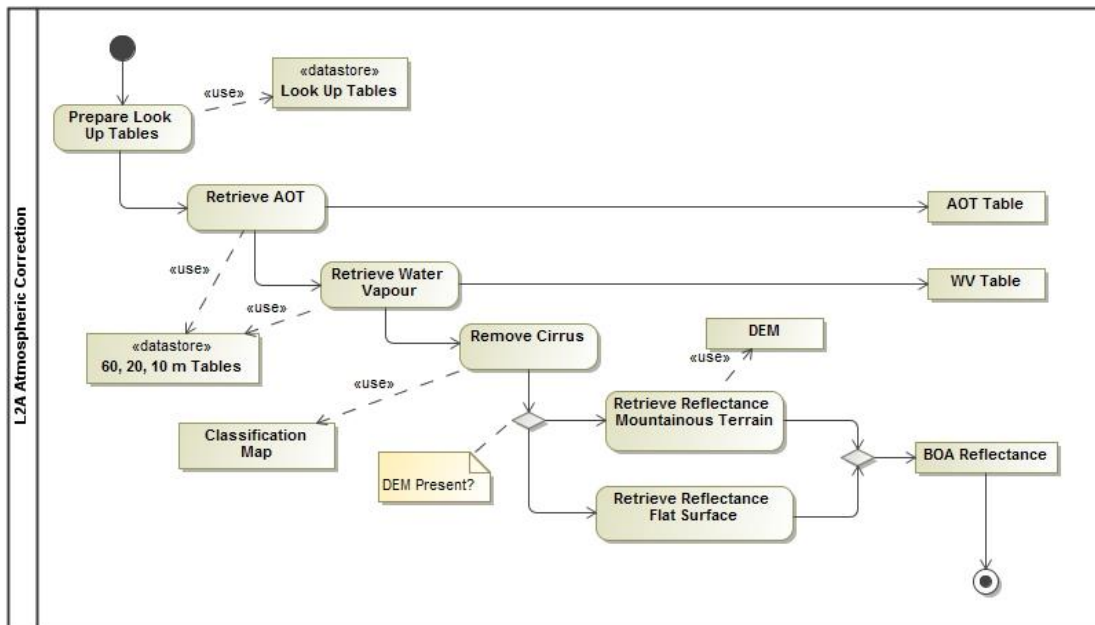


Figure 16: Processing flow for atmospheric correction of Sentinel-2A products (Müller-Wilm, 2016)

### 4.3 Landsat 8 data processing

All Landsat 8 data that was used was of level L1T. The data does not contain reflectance values yet, but it contains Landsat Digital Numbers. Thus this had to be transformed to TOA reflectances first. The data also had to be corrected for other effects. It is possible to do this in QGIS with a plugin called the Semi-Automatic Classification Plugin (SACP). The correction in QGIS is done with the DOS 1 method, which stands for Dark Object Subtraction 1. This is done because dark objects have zero reflectance, but these objects get a reflectance value due to atmospheric scattering. This is necessary in order to use the Landsat 8 data (Gilmore et al., 2015). This was done for all bands independently, after which all bands were stacked in one raster image in QGIS. This method is slightly different than the approach for Sentinel-2 data, where TOA reflectance is then further processed to BOA reflectance. For the purpose of this research it is assumed that

these two slightly different methods will not have a big impact on the results and therefore that the difference is negligible.

#### 4.4 Snowline detection

First of all, the snowline can be derived by visually assessing the satellite images. This can be done by distinguishing between the different colours of snow and ice on the images, on the condition that the image is clear enough, which is not always the case. This is a very easy method, because one can just check this and does not need (advanced) software for this. From here on, it is possible to start developing different methods to derive the snowline from the data. In order to find a snowline, it is helpful to use ASTER GDEM data (or any other DEM) combined with the GLIMS glacier mask to see how a glacier advances; this is sometimes difficult to see from just spectral data. An example of a snowline is given in figure 17.

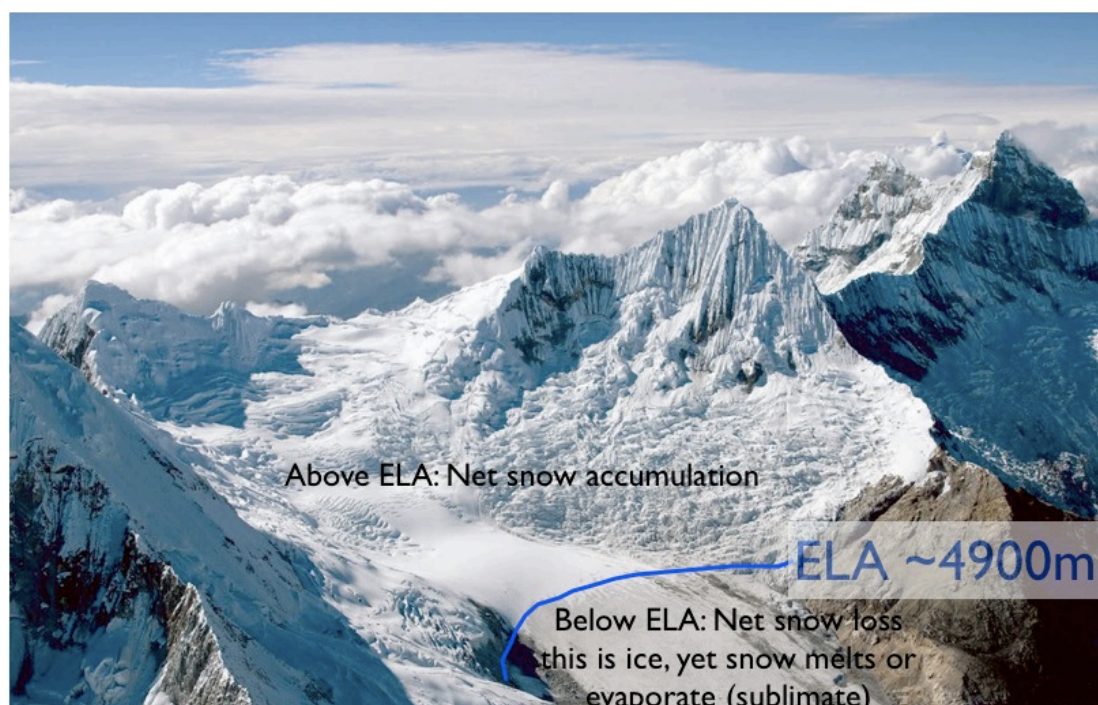


Figure 17: Example of an ELA in the Andes mountain range (National Geographic, 2007)

#### 4.5 Superimposing ASTER GDEM v2 with Sentinel-2 data

Elevation data is useful in order to assess snowlines or to see the course of the glacier. This is done with ASTER GDEM v2 in the Sentinel-2 toolbox. However, due to licensing issues from the ASTER data it is not possible at the time of writing to do this automatically in the Sentinel-2 toolbox. It is possible to do this manually if one manually downloads the ASTER GDEM data and puts it in the hidden folder `$username$/.snap/auxdata/dem/ASTER 1 sec GDEM`, on the condition that the file has the original filename of the ASTER data, i.e. `ASTGTM2_N34E71_dem.tif` and `ASTGTM2_N3471_num.tif`. Once this is done, one can easily add the elevation by choosing Raster -> DEM tools -> Add elevation band -> ASTER 1 sec GDEM in the Sentinel-2 toolbox. The Sentinel toolbox then automatically cuts the ASTER data to the size of the product. An image of Sentinel-2 data next to ASTER GDEM is shown in figure 18.

Combined, it is possible to extract the height of the snowline of a glacier. This is done in two ways in this research. The first is to use the pixel info and extract the height of the snowline. This method is a very simplistic. The second method is to use the Profile plot in SNAP that gives the elevation profile of the snowline. This is also a rather simplistic method, however it takes a bit more time, as one has to define the geometry of the snowline.

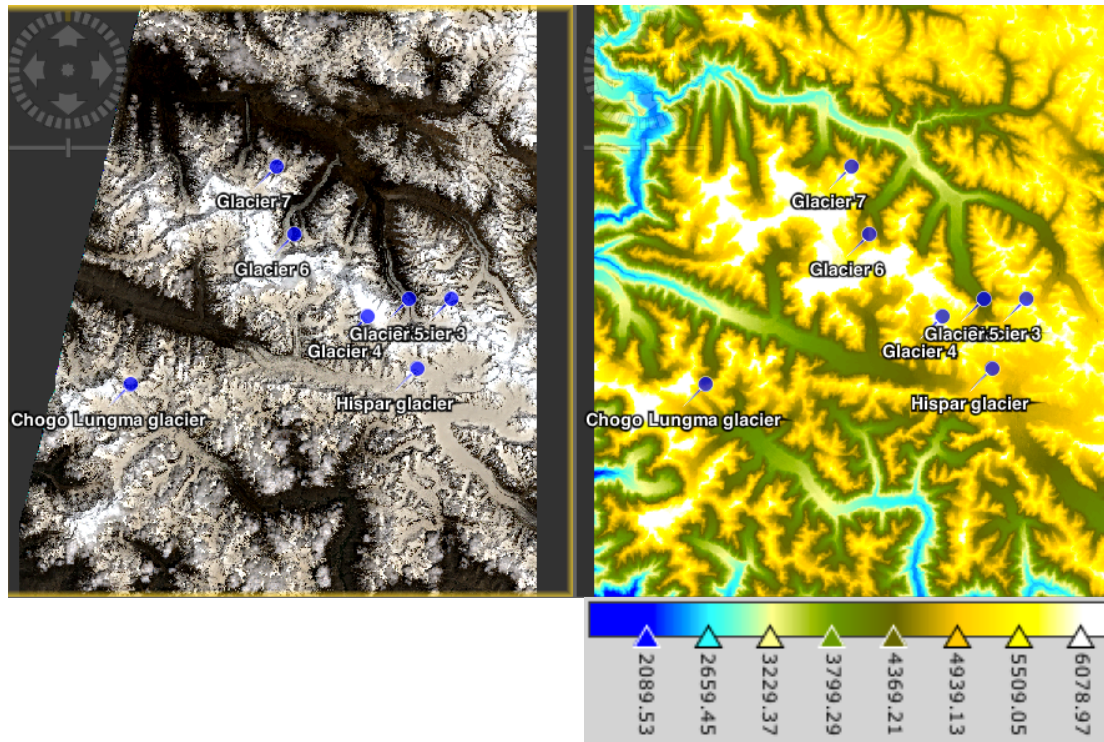


Figure 18: Sentinel-2 data combined with ASTER GDEM v2, together with the legend

#### 4.6 NDSI

Another method to distinguish snow on a glacier is the Normalised-Difference Snow Index. As mentioned earlier, snow is highly reflective in the visible part of the electromagnetic spectrum (see figure 3) and highly absorbing in the NIR/SWIR part of the spectrum. In Sentinel-2 data, the NDSI is calculated by using equation 4.1. In case of Landsat 8 data, the NDSI is calculated with a different band combination as seen in equation 4.2. In general, the NDSI has the form:  $(\text{Green band} - \text{SWIR band}) / (\text{Green band} + \text{SWIR band})$ . A figure of a map showing the NDSI next to Sentinel-2 data is shown in figure 19.

$$NDSI(\text{Sentinel} - 2) = \frac{(B3 - B11)}{(B3 + B11)} \quad (4.1)$$

$$NDSI(\text{Landsat } 8) = \frac{(B3 - B6)}{(B3 + B6)} \quad (4.2)$$

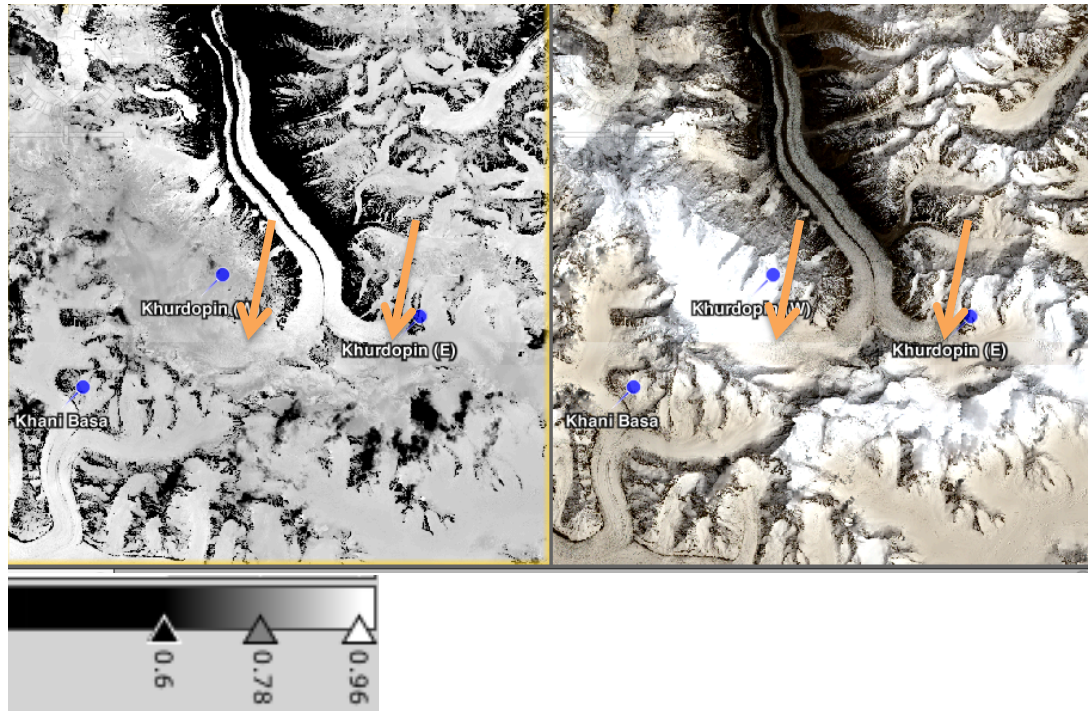


Figure 19: NDSI with colour legend (left) and Sentinel-2 RGB image from the Khurdopin glacier, zoom 1:51.0, the orange arrows indicate the snowline (snowline determination was done at a higher zoom)

#### 4.7 Band combinations

When an image is created, the bands and band combinations can be modified. This is done to highlight different types of land cover, as each type of land cover has a different reflectance in different bands. By highlighting different bands in an RGB image, thus by modifying the bands shown as RGB in an image, snow and ice can be detected. In Landsat TM this is done by using the band combination 4,5,7 as RGB (Parece et al., 2015). This translates to Sentinel-2 bands 8A, 11 and 12 respectively and for Landsat 8 data this becomes band combination 5,6,7. Clouds, snow and ice can be distinguished and snow/ice is shown in red. In a study similar to this one, Portengen used band combination 5,4,3 for Landsat 7 ETM+ and Landsat 8 images. Information on the bands of Landsat can be found in section 3.5. This can be translated to Sentinel-2 bands and this results in a band combination of bands 11,8A,4 as RGB for the method by Portengen and a band combination of 8A,11,12 as RGB for the method proposed by Parece et al.

Another band combination that can be used for snow/glacier mapping is the Landsat 7 ETM+ combination of bands 5,4,2 as RGB, which maps snow as light blue, glaciers as darker blue and healthy vegetation in bright green (NASA, 2008). This translates to the band combination 11,8A, 3 in Sentinel-2 images. All possible combinations are shown in table 5.

**Table 5: Possible band combinations for snow/ice mapping (designated as R,G,B)**

<b>Method</b>	<b>Landsat TM</b>	<b>Landsat 7 ETM+</b>	<b>Landsat 8</b>	<b>Sentinel-2</b>
Parece et al.	4,5,7	4,5,7	5,6,7	8A,11,12
Portengen	5,4,3	5,4,3	6,5,4	11,8A,4
NASA	5,4,2	5,4,2	6,5,3	11,8A,3

All methods use the spectral response of snow and ice in their designated bands in the RGB image. The difference between the method by Portengen and NASA is that the blue colour in the image is designated to band 4 (665 nm, red colour) or to band 3 (560 nm, green colour). This gives a slight change in colour, but there are no drastic differences. The method by Parece et al. is slightly different, as it switches bands 8A from green to red and band 11 from red to green. Also, it has band 12 (2190 nm, SWIR) as the third band. This does not change much in the type of vegetation mapped, which is still snow/ice. However, the colour in which it is mapped changed changes, because snow/ice is shown in red in this method instead of blue, like in the methods by NASA and Portengen.

#### **4.8 Spectral information of snow and ice in Sentinel-2 data**

The spectral information of different land covers can also be assessed in the Sentinel-2 Toolbox. This can be useful as dirty ice and fresh snow have different albedo and spectral responses. To see whether this is true and how this differs for a couple of different land covers, a supervised classification was done. Five different classes have been used in the area of interest: clouds, snow, dirty ice, ice and bare soil.

## 5. Results

### 5.1 Data processing results

First of all, the products that were used had to be processed. Here the subscenes will be presented for both Sentinel-2 datasets will be shown along with the Landsat 8 images. The processed images of the both areas (first and second dataset) are shown in the Appendix 1. A zoomed in image (1:25.8) plus a scene classification of the first dataset of Sentinel-2 (December 2015) is shown in figures 20 & 21.



Figure 20: Zoomed in RGB image (4,3,2) of the first Sentinel-2 dataset

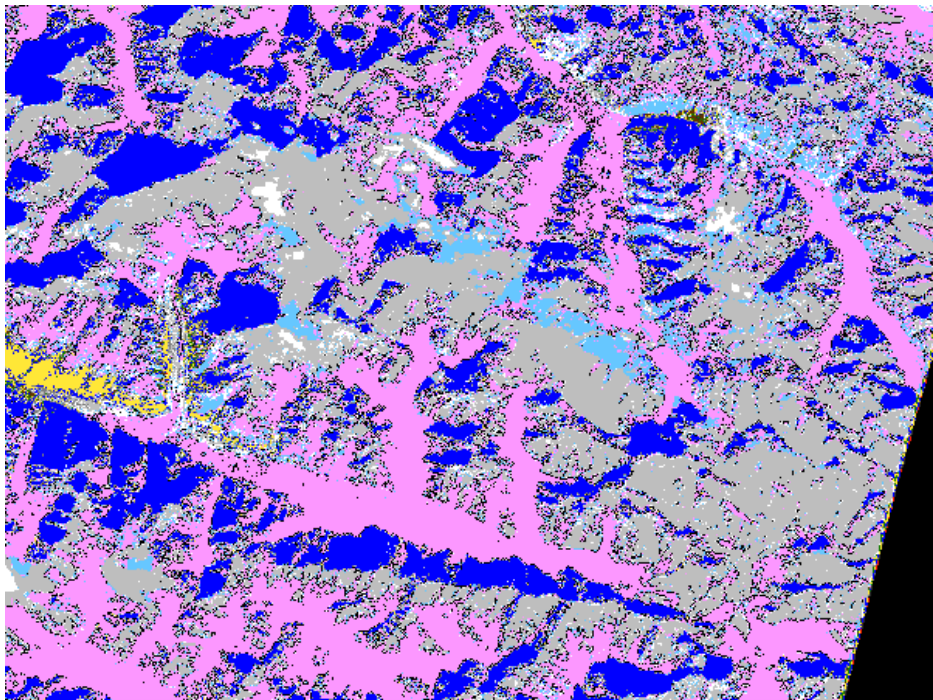


Figure 21: Zoomed in scene classification of first Sentinel-2 dataset (legend is shown in figure 14)

Due to the bad image quality, this dataset was discarded, as no definite conclusions can be drawn from this image. A second dataset was found and cropped to a size that includes a lot of glaciers. The pre-processed image can be seen in figure 22 and the post-processed image can be seen in figure 23. Immediately clear is that the colour of the glaciers changes. This is due to the conversion from TOA reflectance to BOA reflectance, which is done by the Sen2Cor processor.



**Figure 22: Pre-processed Sentinel-2 image of glaciers in the Karakoram (Level-1C, RGB = 4,3,2), zoom 1:306.2**



**Figure 23: Post-processed Sentinel-2 image of glaciers in the Karakoram (Level-2A, RGB=4,3,2), zoom 1:306.2**

## 5.2 Sentinel-2 compared with Landsat 8

In order to compare Sentinel-2 with Landsat data, the images were cropped to a small area of glaciers, including the Hispar glacier as reference point. Various zoomed in images have been made in order to spot the differences between the two datasets. The main focus will be on two large glaciers, which were clearly visible in both datasets, the Hispar glacier and the Chogo Lungma glacier. The Chogo Lungma images can be found in Appendix 1, the zoomed in images of the Hispar glacier are shown in figure 24 and 25.



Figure 24: Sentinel-2 image of the Hispar glacier and surroundings, zoom 1:47.3



Figure 25: Landsat 8 image of the Hispar glacier and surroundings, zoom 1:47.3

The main difference between the Sentinel-2 and Landsat 8 image is the colour of the glaciers. This has probably got to do with the method of processing (Sentinel-2 is processed from TOA to BOA, Landsat 8 was not processed to BOA). Also, the Landsat 8 image is cloudier.

Figures 26 and 27 show a close-up of the end of the Hispar glacier, both indicated previously with a blue arrow in figures 24 and 25.



Figure 26: Sentinel-2 image of the end point of the Hispar glacier, zoom 1:13.4

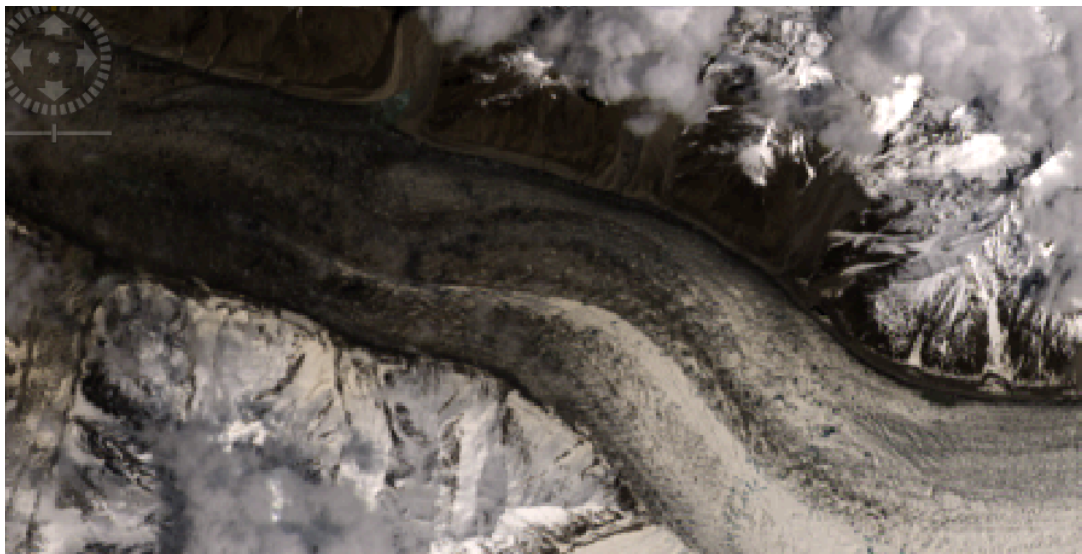
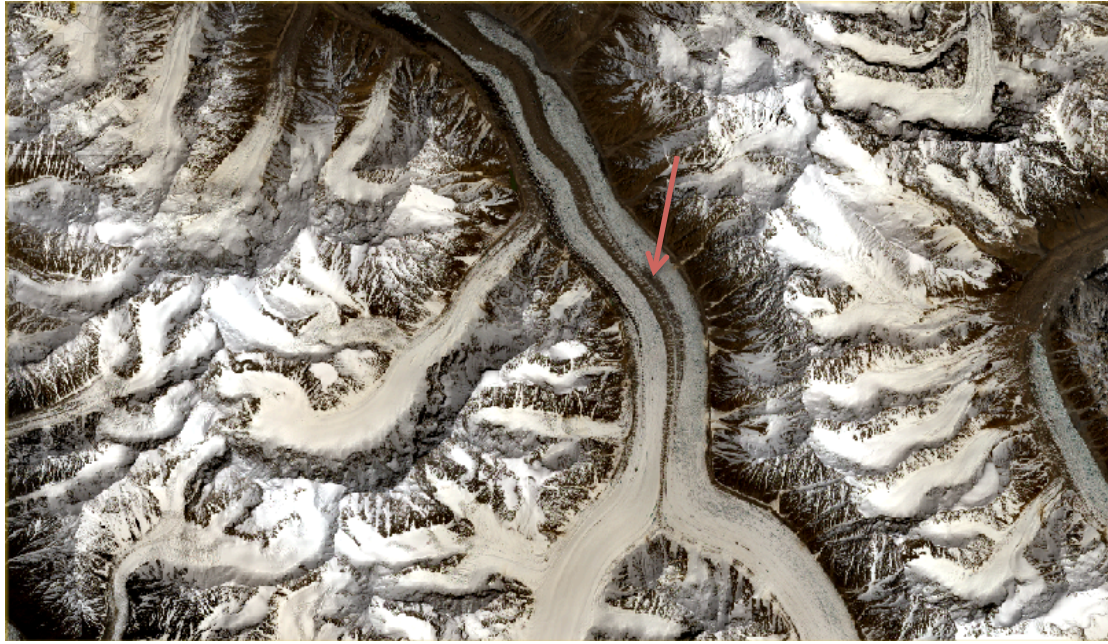


Figure 27: Landsat 8 image of the end point of the Hispar glacier, zoom 1:13.4

A clear difference can be seen in the Sentinel-2 (figure 26 ) and Landsat 8 (figure 27) zoomed in image of the Hispar glacier. First, in the Landsat 8 image there are more clouds, but the resolution in the Sentinel-2 image is a lot higher. The transition from snow/ice to debris is seen a lot sharper and in more detail in the Sentinel-2 image.

A glacier just north of the Hispar glacier is shown as a Sentinel-2 and a Landsat 8 image in figures 28 and 29. A clear medial moraine can be seen here, indicated with a red arrow.



**Figure 28: Sentinel-2 image of a glacier north of the Hispar glacier, the medial moraine is indicated with a red arrow, zoom 1:28.0**



**Figure 29: Landsat 8 image of a glacier north of the Hispar glacier, zoom 1:28.0, the medial moraine is indicated with a red arrow**

Again, the difference between landsat 8 and Sentinel-2 is clearly seen in the resolution of the images. Sentinel-2 provides a much sharper image.

Two images of the Yukshin Garden glacie, showing crevasses in great detail are shown in Appendix 1, in figures 30 and 31. It is immediately clear that crevasses are seen in a much greater detail in the Sentinel-2 images. The Landsat 8 image contains some clouds, but it is clear enough to see that the resolution of the image is a lot lower.



Figure 30: Crevasses (indicated with orange arrow) in the Yukshin Garden glacier on Sentinel-2 imagery, RGB image, zoom 1:10.9



Figure 31: Crevasses in the Yukshin Garden glacier on Landsat 8 imagery, RGB image, zoom 1:10.9

### 5.3 Snow/ice mapping with band combinations

Several methods have been described (section 4.7) to map snow and ice in Sentinel-2 data by using the spectral properties explained in section 2.2 and figure 3. The results of NASA's method are presented in figure 32 and 33; the other two methods (Portengen & Parece et al.) are shown in figures 34 and 35 (Portongen) and figures 36 and 37 (Parece et al.). It is clear that the glaciers are mapped pretty well in all three methods, as the glacier mask overlaps with the glaciers seen in the figures. However, the parts of glaciers where there is more debris present are not mapped well. This goes for all three methods.

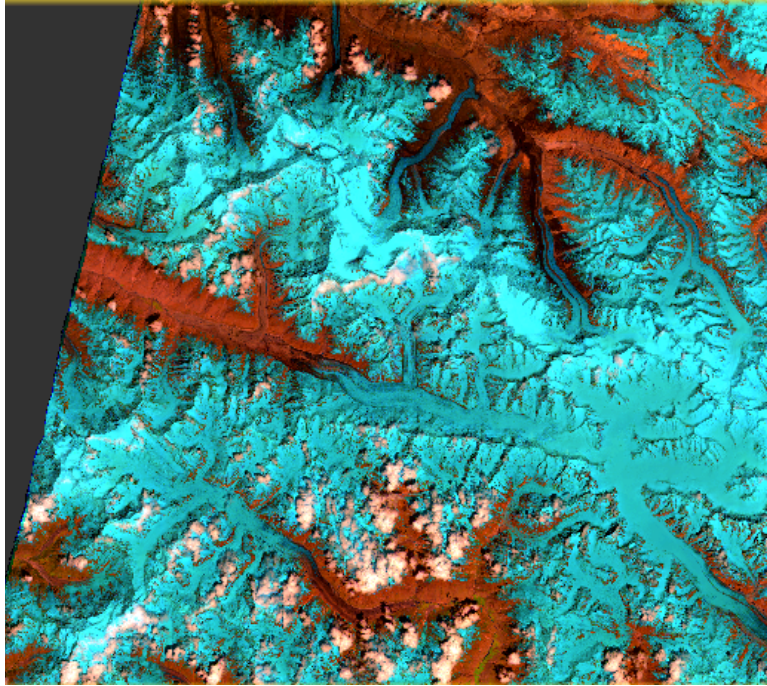


Figure 32: Sentinel-2 false colour image (bands 11,8A,3 as RGB), zoom 1:168.5

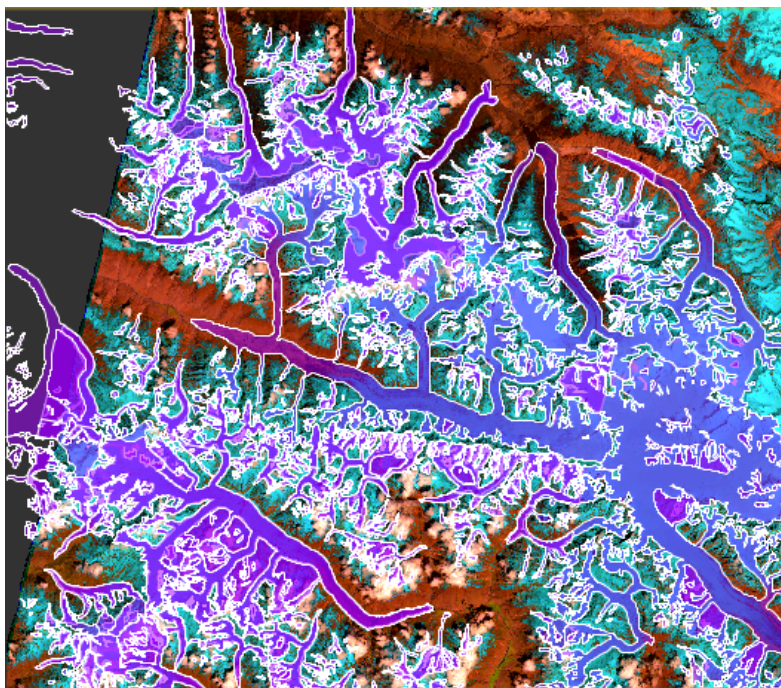


Figure 33: Sentinel-2 false colour image (bands 11,8A,3) with GLIMS glacier mask (purple polygons)

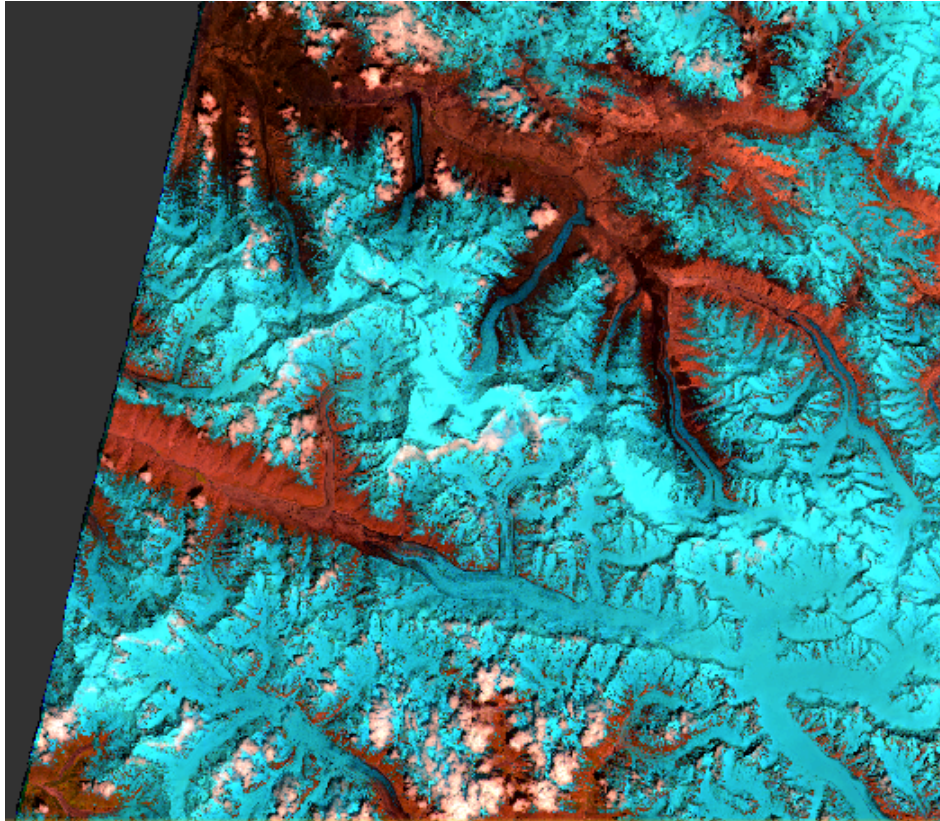


Figure 34: Sentinel-2 false colour image (bands 11,8A,4), zoom 1:168.5, method by Portengen (snow/ice = blue)

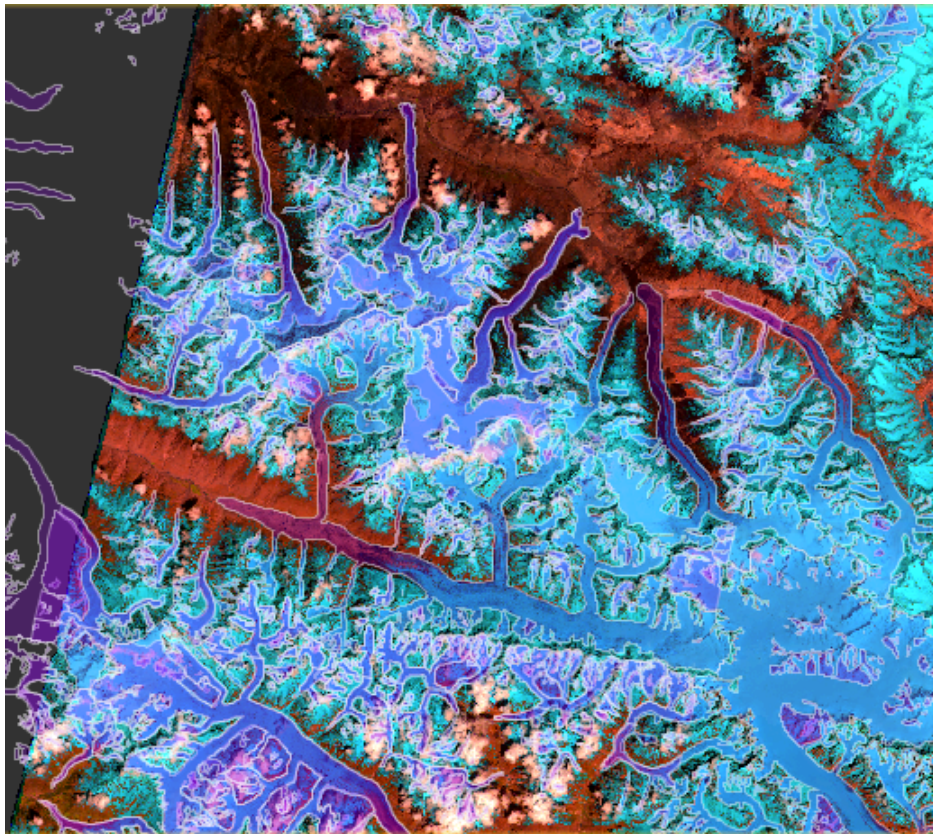


Figure 35: Sentinel-2 false colour image (bands 11,8A,4) including the GLIMS glacier mask (purple polygons), zoom 1:168.5, method by Portengen (snow/ice =blue)

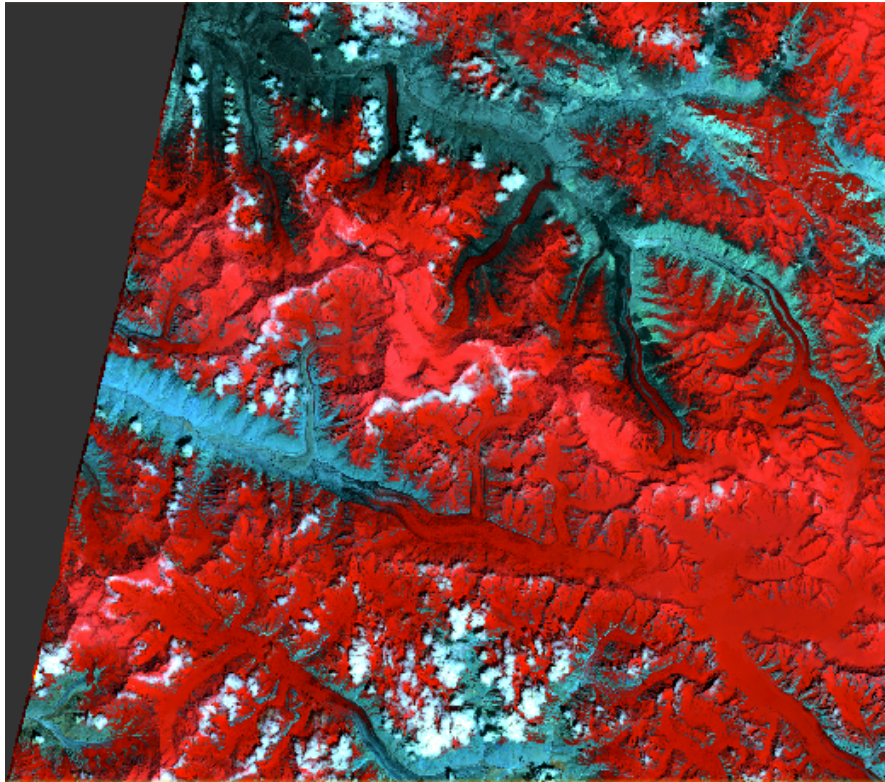


Figure 36: Sentinel-2 false colour image (bands 11,12,8A), zoom 1:168.5 (snow/ice = red), method by Parece et al.

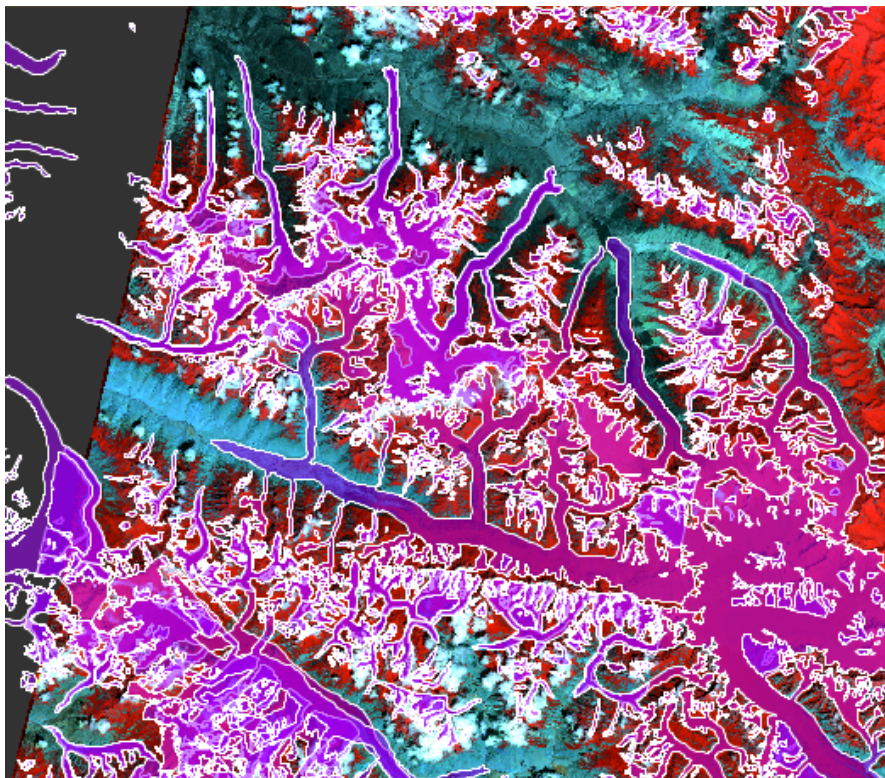


Figure 37: Sentinel-2 false colour image (bands 11,12,8A), zoom 1:168.5, including the GLIMS glacier mask (purple polygons), method by Parece et al. (snow/ice = red)

The spectral signatures in Sentinel-2 of a supervised classification are given in figure 36. The dots represent the locations of the bands in Sentinel-2, as explained in section 3.2. It is clear that ice (yellow) has a different spectral response than dirty ice (red) and snow (purple). This can be seen in the intensity of the response, but also in the shape of the response. Snow responds different than ice between 700 – 900 nm, with the peak shift at 842 nm in particular, as shown with the blue arrows in figure 38. However, the bands before 842 nm also exhibit slightly different behaviour.

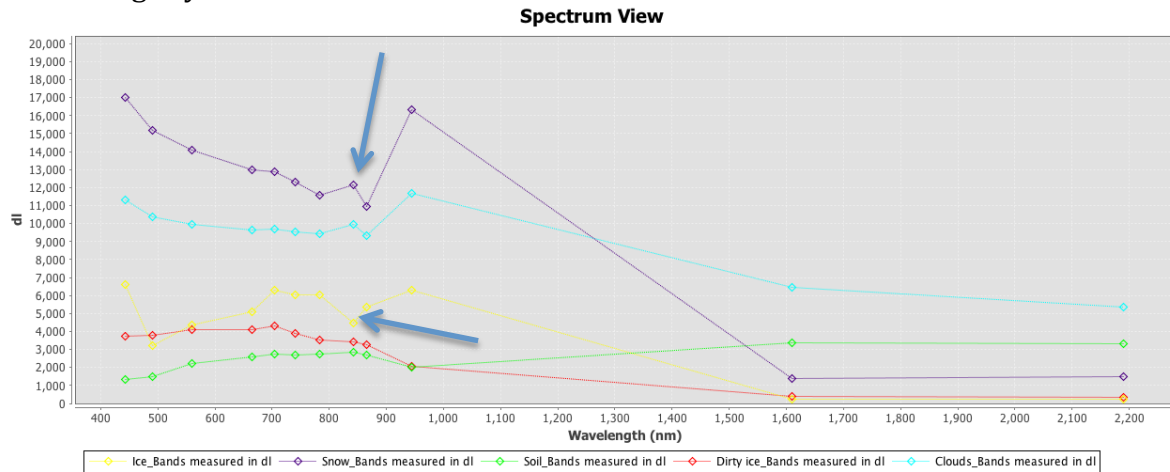


Figure 38: Spectral signature of ice (yellow), snow (purple), soil (green), dirty ice (red) and clouds (light blue)

## 5.4 Snowline determination

In order to determine snowlines, the area has been visually inspected in different band combinations, together with the NDSI method. This lead to several snowlines on different glaciers, the locations of the glaciers are shown in figure 39. The heights of the snowlines have been extracted in two ways: manually and by a height profile plot. The results are plotted in table 6. Zoomed in images of the snowlines are shown in Appendix 2.

Table 6: Snowlines from different glaciers extracted from Sentinel-2 images. Reference height is from Hewitt (2013).

Glacier	Orientation	Quality snowline (1-10)	Height snowline (pixel info, in m)	Height snowline (contour plot, in m)	Glacier name	Reference height in m
1	W-E	7	4880	4900	Chogo Lungma	4800
2	E-W	9	4985	4980	Hispar	4800-5000
3	SE-NW	9	5045	5040	Khurdopin (West)	5000
4	N-S	9	4680	4680	Khani Basa	-
5	SW-NE (variable)	8	5198	5211	Khurdopin (East)	5000
6	SW-NE	8	5566	5520	Yazghil	5000
7	SSE-NNW	9	5305	5285	Malangutti	5000

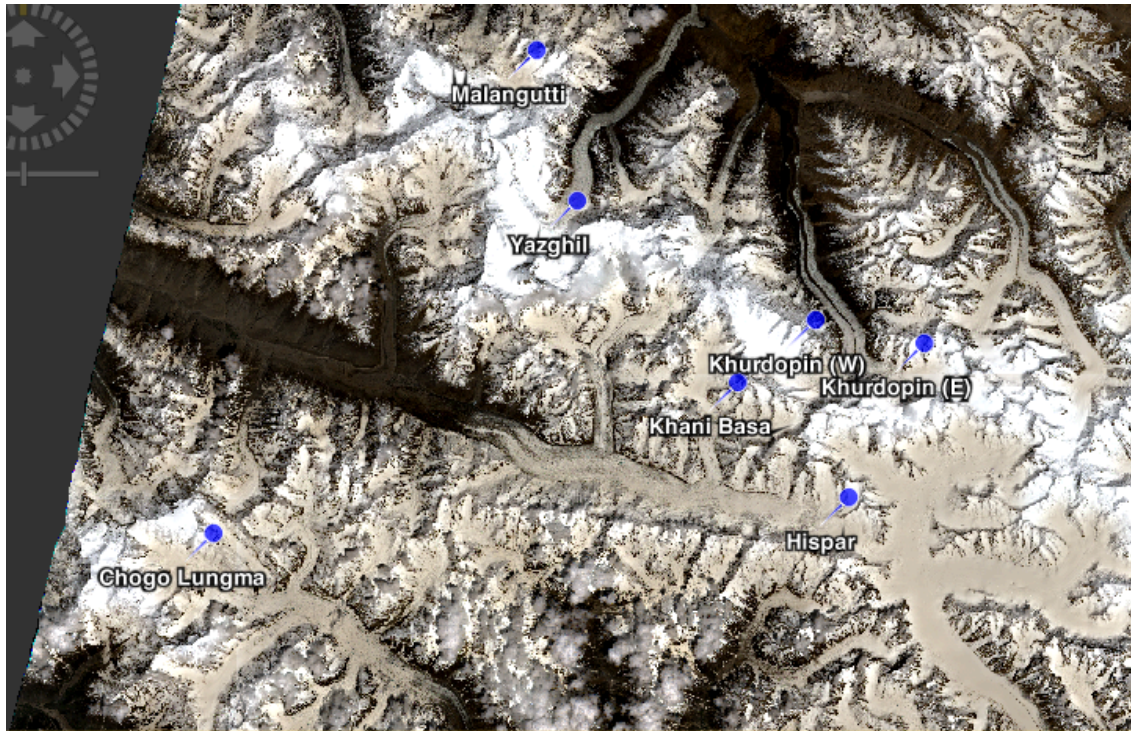


Figure 39: Location of the studied glaciers in an RGB image, zoom 1:121.1

## 6. Discussion

### 6.1 Processing problems

During processing the obtained Level-1C products to a Level-2A product, some problems occurred when the data was processed to 10m resolution. The processor would quit before the job was done. However, when opening the product in the Sentinel-2 Toolbox at a 10m resolution, no errors occurred and images could be obtained that show more detail than a regular Landsat 8 image.

Some other problems that have occurred had to do with instability of the software (Sentinel-2 Toolbox) and with instability of the data hub, from which the required data had to be downloaded. This will gradually improve as both platforms are still under development. Furthermore, better datasets became available during the end of this research, but time did not allow this to be processed and analysed.

Some other interesting features in the Sentinel-2 images are the some bands that can be seen in figure 40. A vertical band of different colour can be seen figure 40, located to the left of the orange arrow. This is probably due to the problems that still occur in processing the Sentinel-2 data from a level-1C to a level-2A product. This does not occur in the Landsat 8 image (figure 41) of the same area, making it more likely that something went wrong during processing. Furthermore, there is another small difference in the images of the Chogo Lungma glacier, all indicated with orange arrows in the images. In the Sentinel-2 image there is some kind of shadow on the glacier, most likely to be a cloud. In the Landsat 8 image there is a small feature seen (indicated with the orange arrow), which cannot be seen on the Sentinel-2 image. This probably is debris or a spot that is not covered by snow at that time. This is possible since the images were shot two weeks from each other.



Figure 40: Sentinel-2 RGB image of the Chogo Lungma glacier



Figure 41: Landsat 8 RGB image of the Chogo Lungma glacier

### 6.2 Differences between the first and second Sentinel-2 dataset

The first Sentinel-2 dataset dating from December 2015 shows quite some glaciers clearly. However, extracting snowlines and other features on the glaciers is still difficult. In figure 20, one clearly sees a lot of shadows that distort the view. Also, on locations where snow is expected (at the start of the glacier), it is difficult to see the transition sometimes due to oversaturated parts in the image. Furthermore, when one looks at the scene classification that is made by the Sen2Cor processor, dark blue colours are all over the place, which would be water. However, this is very unlikely as these locations coincide with the locations of the shadows in the original RGB image. A likely explanation for this is the fact that the obtained dataset dates from 03-12-2015, whereas the first datasets became available at 27-11-2015. Thus the oversaturation and shadows are probably due to sensors that had not been calibrated properly yet at that time. Furthermore, when one takes a closer look at figure A1 of the first dataset in Appendix 1, it is clear that not all individual granules have been processed correctly, as seen in the upper right and left corner.

The more recent Sentinel-2 dataset can also be found in Appendix 1, figures A3 and A4. The location is slightly more to the east, but it also covers the Hispar glacier in the western part of the image. Here it is clear that all problems that have been encountered previously, have disappeared. There are no problems with shadows or oversaturation here. Also, the scene classification provides a much more accurate classification than the algorithm did in the first dataset, as no more water bodies are indicated at locations of shadows for example.

### 6.3 Comparison between Landsat 8 and Sentinel-2

When one looks at Landsat 8 and Sentinel-2 images of the same area, it is immediately clear that both show different colours on glaciers. This is probably due to the different bands (central wavelength and bandwidth) of both instruments. Another reason can be the applied processing method, Sentinel-2 data has been corrected from TOA to BOA reflectance with the algorithm described in section 4.2.2, while the Landsat 8 data was corrected with the DOS-1 algorithm, which is a different way of correction for atmospheric scattering.

Also, a lot of glacial features (crevasses, (medial) moraines) can be seen a lot sharper in Sentinel-2 data. The Sentinel-2 data clearly has a higher resolution compared to Landsat 8 and it can be used to study glaciers in great detail. Figures 30 and 31 show the difference in sharpness between the two satellites on the Yukshin Garden glacier. It is clear that Sentinel-2 has a big potential to study crevasses (and thus other glacial features as well).

When taking a closer look at the times at which the same location is imaged, it becomes clear that the Sentinel-2 image is always shot within a close time range when compared with a Landsat 8 image. Sentinel-2 images of the same area are shot at roughly the same time of day. At the time of writing, only one of the two Sentinel satellites is operational and therefore the revisit time will become higher in the future, making it an excellent instrument to conduct time series studies with, which can possibly be combined with Landsat 8 images.

#### **6.4 Differences between band combinations**

It is clear that all three different methods map ice and snow pretty well when one superimposes the GLIMS glacier mask on top of the image. However, all three methods do not clearly show the debris on glaciers. It is possible to use all three methods for the purpose of mapping snow and ice. Together with GLIMS this provides an easy way to identify glaciers.

#### **6.5 Snowline determination**

The determination of snowlines was difficult in the first Sentinel-2 dataset, but this was a lot easier in the dataset of Sentinel-2 that dates from May. As seen in table 6, most of the snowline altitudes coincide with literature (Hewitt, 2013). This does not hold for the Yazghil and Malangutti glacier, but this can be because Hewitt states secondary literature dated in between 1959 and 2011. It also coincides with the image presented in figure 6, showing the monsoon and ELAs in the Hindu-Kush Himalayan.

#### **6.6 GLIMS as an incomplete dataset**

It seems that the GLIMS glacier mask is not a complete database and therefore one cannot fully rely on this. Several examples have been found during the study, in which it became clear that some major glaciers are not included in the database, as seen in figure 13. This is just one example, as one zooms in closer on different areas, it became clear that more glaciers were not included in the database.

## 7. Conclusion

Sentinel-2 data is processed to a product giving information on surface reflectance in the Sentinel-2 toolbox with help of the Sen2Cor processor, all freely available from ESA. A different method is to use QGIS to do this, but this takes a lot of time. The processor and the toolbox are not completely operational at this moment, but this will become better in the near future. Handling the size of the images is essential, as it takes a lot of processing power in order to do this in an efficient way. If this is not done, processing and analysing a Sentinel-2 image takes a long time.

Sentinel-2 images provide a sharper view than Landsat 8 images, as expected as the bands have a higher resolution. It provides a look on glaciers from space at an astounding resolution, making it excellent to study individual glacial features. Also, in combination with Landsat 8, the chance of getting cloud free images increases due to the high revisit time of Sentinel-2 and how close the visit time is to Landsat 8 images that are shot of the same area. This makes Landsat 8 and Sentinel-2 an excellent combination to conduct time series studies with. It becomes easier to analyse a glacier advancing/retreating this way, without the need of fieldwork. However, data that was published and transferred in the first phase (December 2015) had issues with processing, such as a lot of shadows and oversaturated pixels in images.

Different methods exist to extract snowlines from satellite imagery. Here, Sentinel-2 images were combined with ASTER GDEM v2 data and the GLIMS glacier mask. Visually assessing the data lead to the determination of the snowlines, making it possible to extract the height with help of individual pixel info. The height can also be extracted with help of the Profile plot, which gives an elevation profile of the snowline. Mapping ice/snow is done in an easy way by creating false colour images with bands that give information about the spectral features of snow and ice. No particular combination is preferred, as long as it is clear that the method of Parece et al. maps snow and ice in red, whereas the other methods map it as blue.

The heights of the snowlines coincide with already available literature (Hewitt, 2013). For example, the snowline of the Chogo Lungma glacier is estimated at 4800m by Hewitt and was found to be at approximately 4880/4900 m in tis research. The snowline of the Hispar glacier is approximated by Hewitt to lay around 4800-5000m. This coincides with the snowline that was found during this research, where it was estimated to lay at 4880/4885 m. This coincides with figure 6, however this is quite a rough estimate since the image shows a large area. Differences are seen in the Yazghil glacier, where Hewitt approximates the snowline to be at an altitude of 5000 m, while the snowline here was found at 5520/5566 m. Differences are also seen in the approximation of the snowline of the Malangutti glacier, Hewitt states 5000 m, while the snowline is located at 5305/5285 m. These differences are probably due to outdated references that Hewitt used.

## 8. Recommendations

Several problems occurred during this research when it comes to handle the size of a Sentinel-2 image. Therefore, it is wise to crop the image to a small area of interest as soon as possible. Sentinel-2 data can be used in larger areas, but depending on the processing power of the computer used, processing and visualising can take a large amount of time. Also, the Sen2Cor processor was not fully operational at 10m resolution. It produced results, but the application would terminate before the end of processing, so some data is missing. Luckily, this was not data that was crucial in this research.

During this research, the idea was to compare the results of Portengen (done with Landsat 8) with the results obtained from Sentinel-2 data. However, no cloud free data was available from the Nyainqêntanglha mountain range at the time of writing. It could be interesting to conduct a time-series study of Nyainqêntanglha (and other areas on the Tibetan Plateau) in future research, due to the high revisit time of the Sentinel-2 constellation if it is fully operational. This would provide an excellent opportunity to study the local climate, seasonal variability in glaciers and to further investigate the Karakoram anomaly (Hewitt, 2005). Furthermore, it is also possible to see the variation in of the terminus of glaciers, to see whether accumulation or ablation dominates. This will also be interesting in climate studies.

It is also possible to process the data in a different way. During the research, the Semi Automatic Classification plugin in QGIS got an update in which it became possible to download and process Sentinel-2 data. The atmospheric correction that would be applied there is done with the DOS subtraction algorithm, similarly to how Landsat 8 was processed in this study. It would be interesting to see how these results compare to the results obtained here. If this method would be done, one could also make supervised classifications in order to detect snowlines and other glacial features. This was not possible in the Sentinel-2 toolbox at the time of writing. Also, it would be interesting to see how professional software, like ENVI, would process Sentinel-2 data and explore how this is different (or if it is easier) than the open-source software used in this study. ENVI probably uses a slightly different module to correct for atmospheric effects, but I think it would be more user friendly. One can switch from the Sentinel-2 toolbox to QGIS after processing, since it is possible to export the cropped product to a GeoTiff format. This was however not part of this project, due to a lack of time since this would be a time-consuming method of working.

The GLIMS glacier mask was also used, but this did not show a difference between snow and ice. Therefore the mask is not usable in determining a snowline, but it can be used to identify glaciers. Another dataset that might be of use is the snow cover product of the Moderate Resolution Imaging Spectroradiometer (MODIS). This product is able to discover snow covered land and even snow-covered ice on inland water. MODIS is an instrument aboard the Terra and Aqua satellites. Together these two satellites map the entire earths surface in 1 to 2 days, while information on the surface is retrieved in 36 spectral bands. However, it must be noted that the highest resolution achieved by MODIS is only 250 m.

## References

14th Session of the WMO Commission for Hydrology, CHy-14. (2012). *Review on remote sensing of the snow cover and on methods of mapping snow*. Retrieved from

[http://www.wmo.int/pages/prog/hwrrp/chy/chy14/documents/ms/remote\\_sensing\\_snow\\_cover\\_methods\\_mapping\\_snow.pdf](http://www.wmo.int/pages/prog/hwrrp/chy/chy14/documents/ms/remote_sensing_snow_cover_methods_mapping_snow.pdf) on 03-06-2016.

Armstrong, R.L. (2010). *The Glaciers of the Hindu-Kush-Himalayan Region: A Summary of the Science Regarding Glacier Melt/Retreat in the Himalayan, Hindu-Kush, Karakoram, Pamir, and Tien Shan Mountain Ranges*. Technical Paper. Kathmandu, Nepal: International Centre for Integrated Mountain Development. Retrieved from [http://lib.icimod.org/record/26917/files/attachment\\_734.pdf](http://lib.icimod.org/record/26917/files/attachment_734.pdf), on 01-06-2016.

Benn, D. I., & Evans, D. J. A. (1998). *Glaciers & glaciation*. London; New York: Arnold; Wiley.

Bolch, T., Kulkarni, A., Kääb, A., Huggel, C., Paul, F., Cogley, J. G., Stoffel, M. (2012). The state and fate of Himalayan glaciers. *Science (New York, N.Y.)*, 336(6079), 310-314.

EarthExplorer, USGS. (2016). Retrieved from <http://earthexplorer.usgs.gov> on June 10, 2016.

ESA. (2016). *Sentinel-2 MSI user guide*. Retrieved from <https://earth.esa.int/web/sentinel/user-guides/> on 02-06-2016.

ESA. (2016). *Sentinel-2-MSI naming convention*. Retrieved from <https://sentinel.esa.int/web/sentinel/user-guides/sentinel-2-msi/naming-convention> on 03-06-2016.

Eumetrain. (2016). Retrieved from [http://www.eumetrain.org/data/3/358/media/images/Fig\\_1\\_1\\_spectrum.jpg](http://www.eumetrain.org/data/3/358/media/images/Fig_1_1_spectrum.jpg), on 3-6-2016.

Floudas, C. A., & Pardalos, P. M. (2009). *Encyclopedia of optimization*. New York, USA: Springer Science & Business Media.

Gilmore, S., Saleem, A., Dewan, A. (2015). Effectiveness of DOS (Dark-Object Subtraction) method and water index techniques to map wetlands in a rapidly urbanising megacity with Landsat 8 data. *Research@Locate '15*, 1323, 100-108. Retrieved from <http://ceur-ws.org/Vol-1323/paper41.pdf>.

Hewitt, K. (2005). The Karakoram Anomaly? Glacier Expansion and the 'Elevation Effect', Karakoram Himalaya. *Mountain Research and Development*, 25(4), 332-340.

Hewitt, K. (2013). *Glaciers of the Karakoram Himalaya : glacial environments*,

*processes, hazards and resources* (pp. 153). Dordrecht, NL : Springer.

Hooke, R. L. (2005). *Principles of glacier mechanics* (2nd ed.). Cambridge, UK: Cambridge University Press.

Jspacesystems. (2016). Retrieved from <http://www.jspacesystems.or.jp/ersdac/GDEM/E/image/5.jpg> on 02-06-2016.

Müller-Wilm, U. (2016). *Sentinel-2 MSI – Level-2A Prototype Processor Installation and User Manual*. Retrieved from <http://step.esa.int/thirdparties/sen2cor/2.2.1/S2PAD-VEGA-SUM-0001-2.2.pdf>, on 01-06-2016.

NASA. (2008, October 6). Most Alaskan Glaciers Retreating, Thinning, and Stagnating, says Major USGS Landsat-Based Report. Retrieved from <http://landsat.gsfc.nasa.gov/?p=565> on 06-06-2016.

NASA. (2016). *GDEM*. Retrieved from <https://asterweb.jpl.nasa.gov/gdem.asp> on 02-06-2016.

NASA. (2016). *Landsat 8 bands*. Retrieved from [http://landsat.gsfc.nasa.gov/?page\\_id=5377](http://landsat.gsfc.nasa.gov/?page_id=5377) on 11-06-2016.

NASA. (2016). *Image of the Himalayan/Karakoram*. Retrieved from [http://eoimages.gsfc.nasa.gov/images/imagerecords/82000/82581/himalaya\\_map\\_color\\_lrg.jpg](http://eoimages.gsfc.nasa.gov/images/imagerecords/82000/82581/himalaya_map_color_lrg.jpg) on 27-06-2016.

National Geographic. (2007). *ELA picture*. Retrieved from <http://joannenova.com.au/2010/06/save-the-world-whitewash-the-andes/> on 14-06-2016.

National Research Council. (2012). *Himalayan glaciers : climate change, water resources, and water security*. Washington, USA: National Academies Press.

Parece, T., Campbell, J., McGee, J. (2015). *Remote Sensing Analysis in an ArcMap Environment*. Retrieved from [http://viriniaview.cnre.vt.edu/tutorial/Chapter\\_12\\_Band%20Combinations%20Using%20Landsat%20Imagery.pdf](http://viriniaview.cnre.vt.edu/tutorial/Chapter_12_Band%20Combinations%20Using%20Landsat%20Imagery.pdf) on 07-06-2016.

Portengen, L. (2014). *Landsat derived snowline variations in Nyaingêntanglha Mountains on the Tibetan Plateau* (Bachelor's thesis). Retrieved from <http://rs.tudelft.nl/~rlindenbergh/education/BscThesisLeonoor.pdf>

Rees, W.G. (2013). *Physical principles of Remote Sensing*. New York, USA: Cambridge University Press.

Singh, V. P., Singh, P., & Haritashya, U. K. (2011). *Encyclopedia of snow, ice and glaciers*. The encyclopedia of earth sciences series; Encyclopedia of earth

sciences series (Springer (Firm)), Retrieved from ebrary  
<http://site.ebrary.com/id/10480367>  
SpringerLink <http://dx.doi.org/10.1007/978-90-481-2642-2>  
Ebook Library  
<http://public.eblib.com/choice/PublicFullRecord.aspx?p=3066860>

Thayyen, R. J., & Gergan, J. T. (2009). Role of glaciers in watershed hydrology: "Himalayan catchment" perspective. *Cryosphere Discussions*, 3(2), 443-476.

Yao, T., Thompson, L., Yang, W., Yu, W., Gao, Y., Guo, X., Pu, J. (2012). Different glacier status with atmospheric circulations in Tibetan Plateau and surroundings. *Nature Climate Change*, 2(9), 663-667.

## Appendix 1: Data processing and images

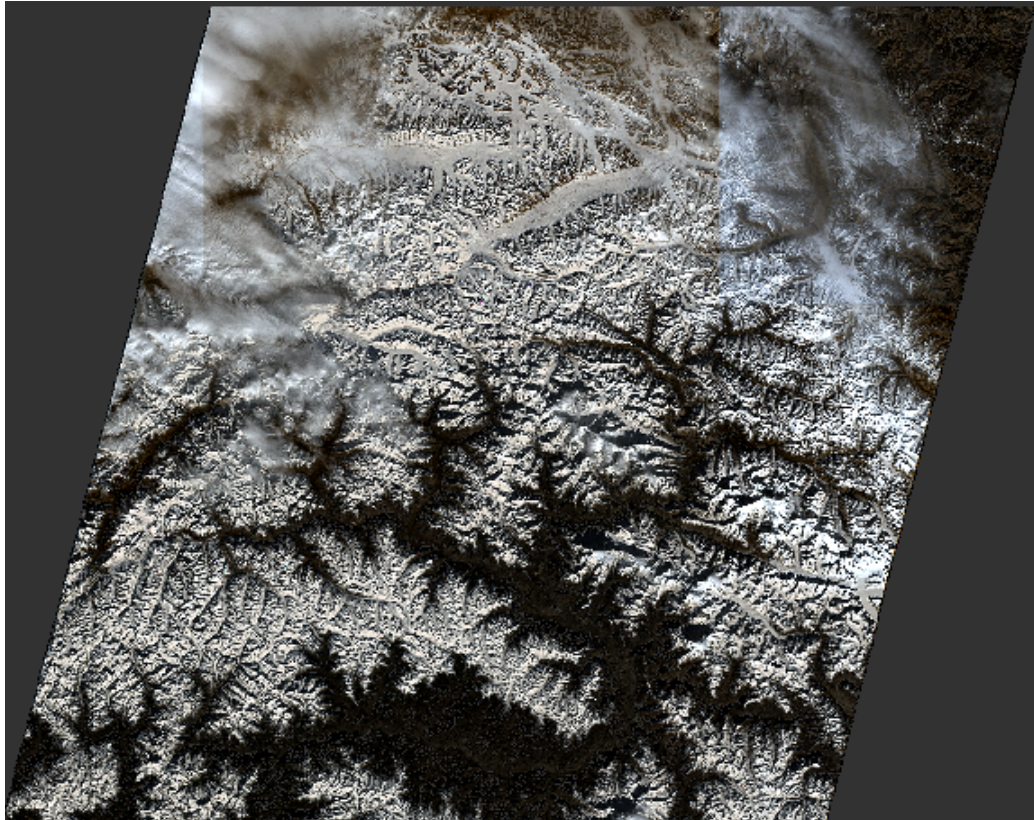


Figure A1: Sentinel-2 dataset RGB image (bands 4,3,2), dated 3 December 2015

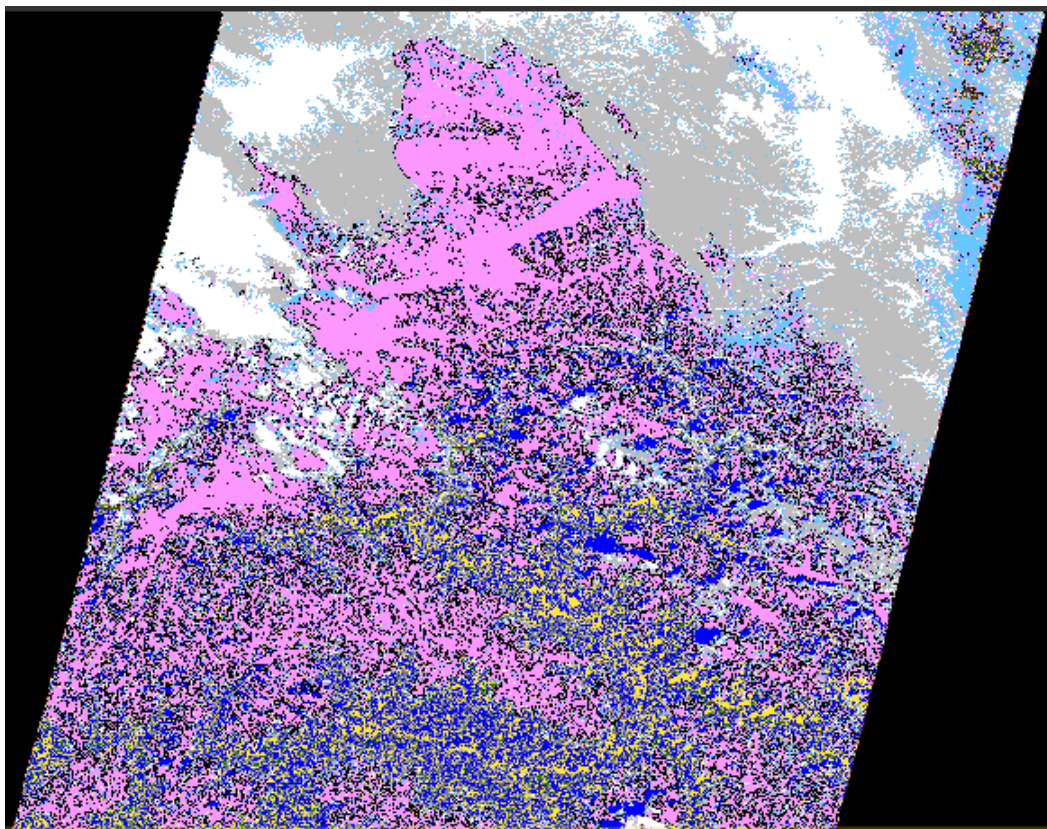


Figure A2: Scene classification (SC) of Sentinel-2 dataset, dated 3 December 2015

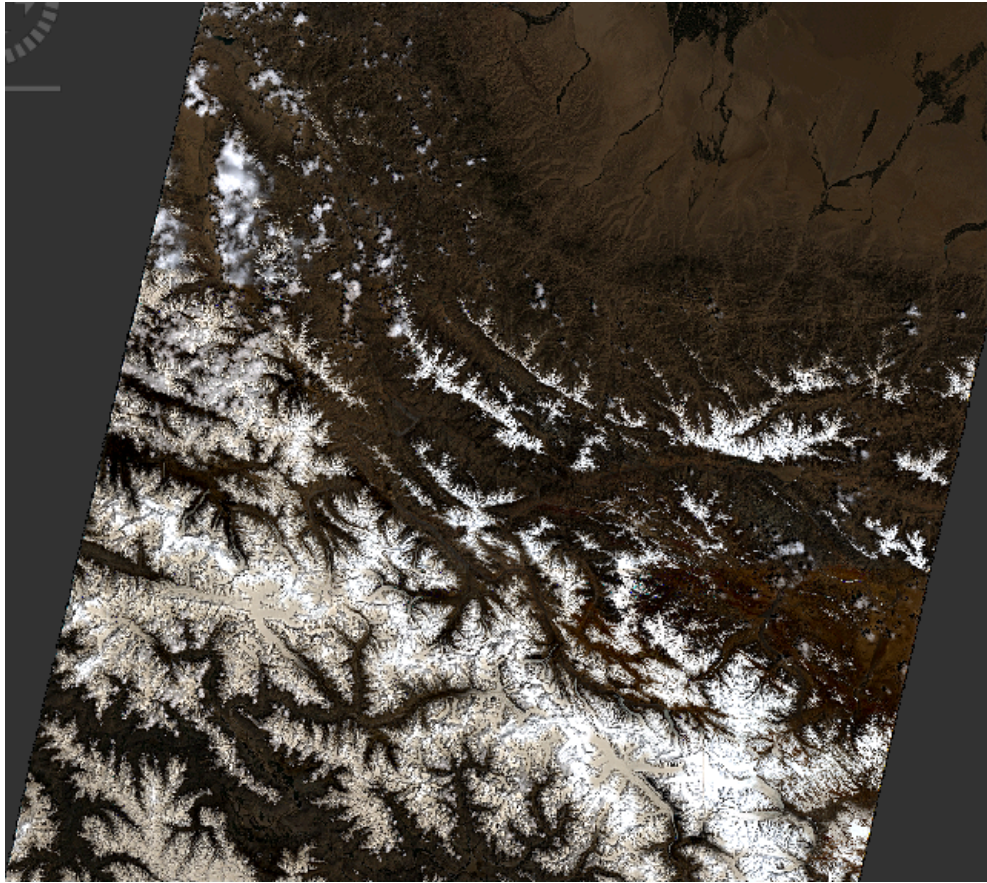


Figure A3: Sentinel-2 dataset RGB image (bands 4,3,2), dated 18 May 2016

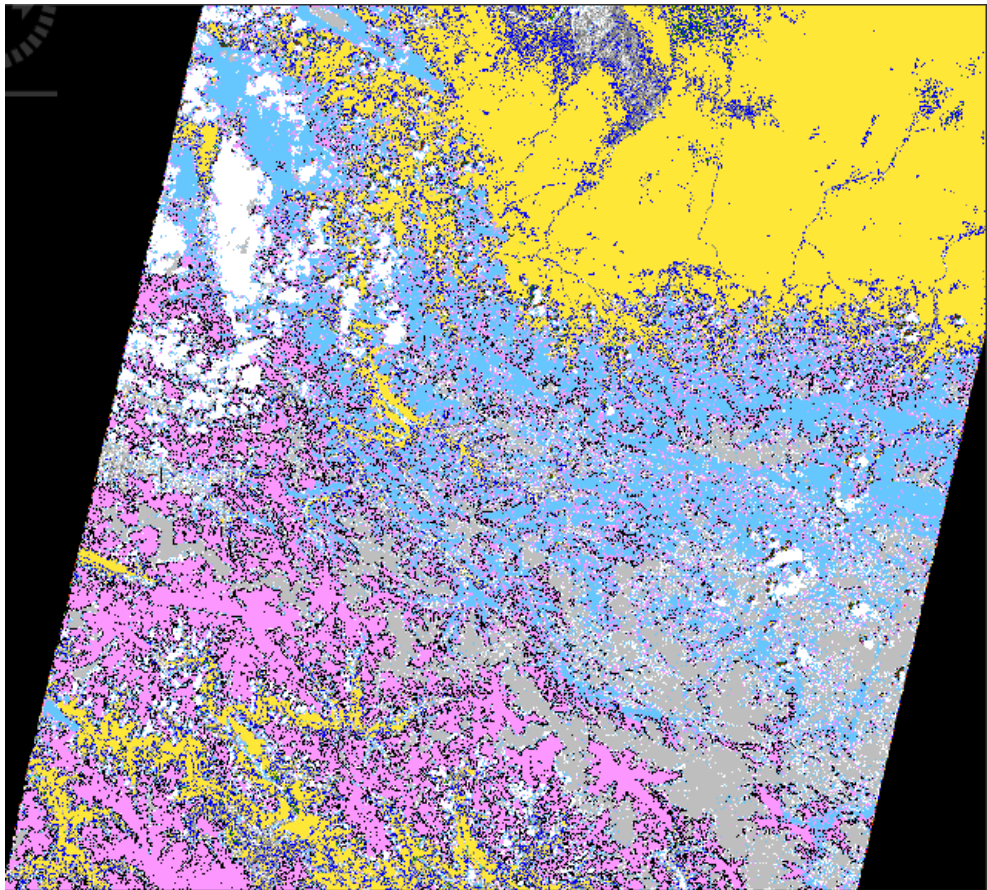


Figure A4: Scene classification (SC) of Sentinel-2 dataset, dated 18 May 2016

## Appendix 2: Zoomed in images of snowlines

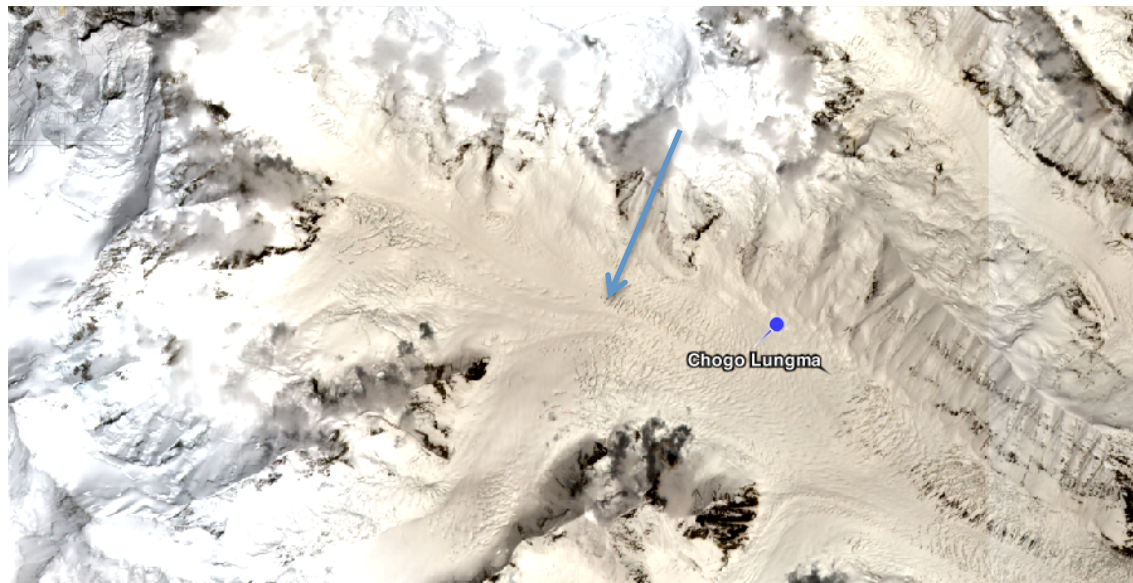


Figure A5: Snowline (blue arrow) of the Chogo Lungma glacier in Sentinel-2 (bands 4,3,2 as RGB), zoom 1:12.8



Figure A6: Snowline (blue arrow) of the Yazghil glacier in Sentinel-2 (bands 4,3,2 as RGB), zoom 1:13.3



Figure A7: Snowline (blue arrow) of the Hispar glacier in Sentinel-2 (bands 4,3,2 as RGB), zoom 1:16.9

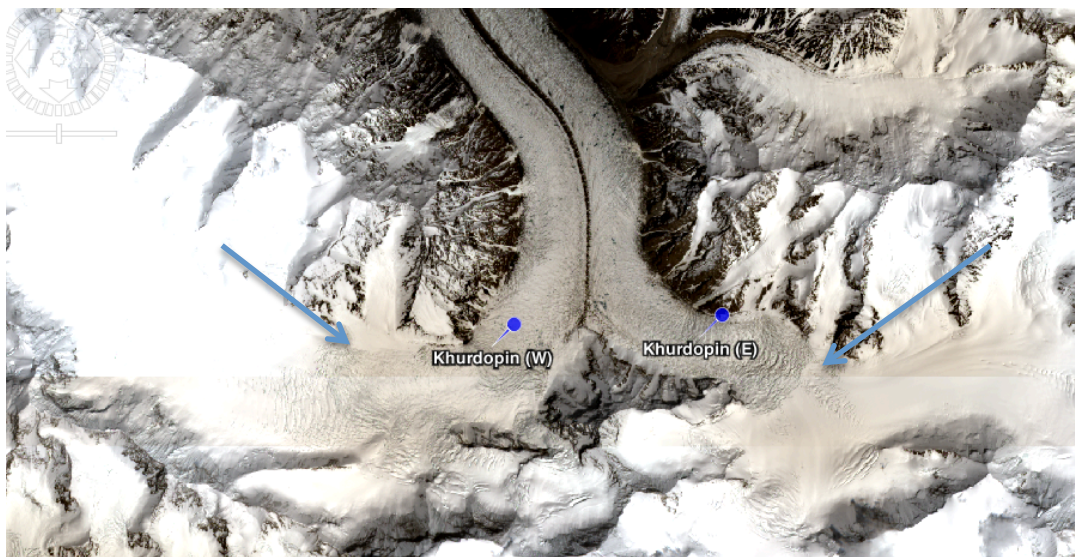


Figure A8: Snowlines (blue arrows) of Khurdopin (E) and Khurdopin (W) in Sentinel-2 (bands 4,3,2 as RGB), zoom 1:17.6

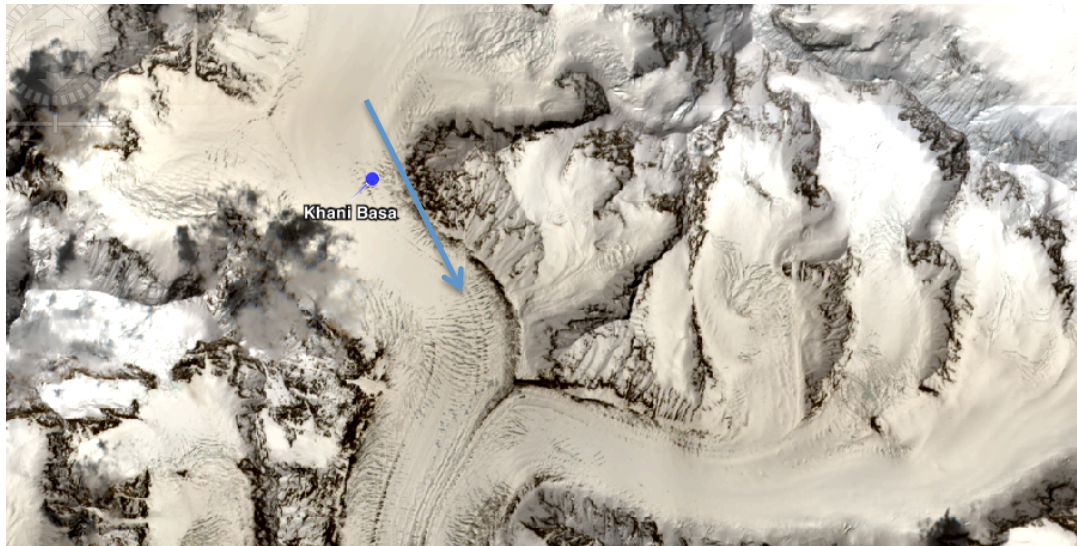


Figure A9: Snowline (blue arrow) of the Khani Basa glacier in Sentinel-2 (bands 4,3,2 as RGB), zoom 1:11.2

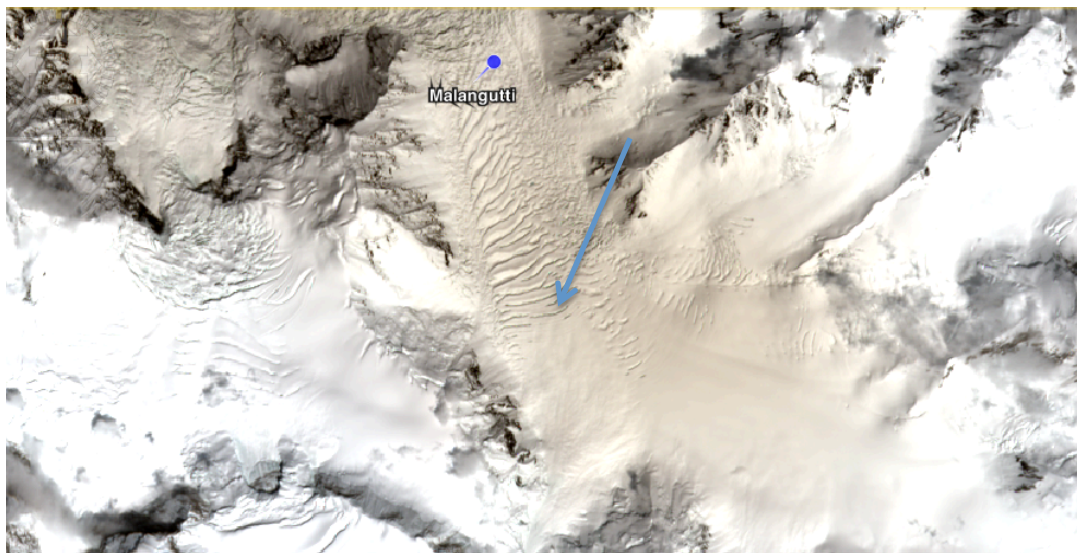


Figure A10: Snowline (blue arrow) of the Malangutti glacier in Sentinel-2 (bands 4,3,2 as RGB), zoom 1:9:0